

NASA Contractor Report 3453

NASA
CR
3453
c. 1

Mathematical Modeling of Damage in Unidirectional Composites



James G. Goree, Lokeswarappa R. Dharani,
and Walter F. Jones

LOAN COPY: RETURN TO
AFWL TECHNICAL LIBRARY
KIRTLAND AFB, TEX.

GRANT NSG-1297
AUGUST 1981

NASA



NASA Contractor Report 3453

Mathematical Modeling of Damage in Unidirectional Composites

James G. Goree, Lokeswarappa R. Dharani,
and Walter F. Jones
Clemson University
Clemson, South Carolina

Prepared for
Langley Research Center
under Grant NSG-1297

NASA

National Aeronautics
and Space Administration

**Scientific and Technical
Information Branch**

1981

SUMMARY

A review of some approximate modeling techniques used to develop analytical solutions for damaged, fiber-reinforced composite materials is presented along with previously unpublished results of the past year's research concerning the application of these methods to particular problems.

The classical shear-lag stress-displacement assumption is fundamental to much of this work. Based on this approximation, solutions are developed for the two-dimensional region containing unidirectional fibers with initial damage in the form of, respectively, a notch, a rectangular cut-out, and a circular hole. An ultimate stress failure criterion is used for both the fibers and the matrix; simple tension for the fibers and shear failure for the matrix. Models which account for longitudinal matrix yielding and splitting as well as transverse matrix yielding and fiber breakage as a function of initial damage, material properties and applied stress are presented. The fibers are taken as linearly elastic and the matrix material as either elastic-perfectly plastic or elastic-strain hardening. A cover sheet constraining the unidirectional laminate is also introduced although only its influence on the unidirectional laminate is modeled; the stresses within the constraint layer are not computed.

For ductile matrix composites (boron/aluminum) the results indicate that longitudinal matrix yielding and transverse notch extension are the most significant forms of damage to include in order for the model to agree with experimental results. The extent of the

stable transverse damage is shown to be approximately constant, independent of initial notch length. Including a cover sheet and/or strain-hardening matrix has minor influence. In the case of brittle matrix composites (graphite/epoxy) longitudinal splitting is shown to be the dominant form of damage.

Very little difference is found between the results for the three types of initial damage, i.e., the notch, rectangular cut-out, and circular hole. In all cases, the presence of additional damage changes the nature of the stress distribution in the unbroken fibers. For the original Hedgepeth problem of a notched laminate the stresses decay as the square root of the distance from the notch tip; including longitudinal or transverse damage significantly reduces the stress concentration and gives a much more uniform stress state in the unbroken fibers. It is shown that this behavior cannot be accounted for by introducing an effective notch length or crack tip damage zone with a square-root behavior.

The formulation of the problem for an edge notch in a unidirectional half-plane with no additional damage is also developed and the appropriate equations are recorded but numerical results are not given. This solution forms the basis for the general problem of adjoining half-planes of different fiber-matrix properties now being developed by the writers.

TABLE OF CONTENTS

| | Page |
|--|------|
| SUMMARY | iii |
| LIST OF FIGURES | vi |
| INTRODUCTION | 1 |
| FORMULATION OF MATHEMATICAL MODELS | 5 |
| A. Two-Dimensional Shear-Lag Model with Broken Fibers | 5 |
| B. Two-Dimensional Shear-Lag Model with Broken Fibers and Longitudinal Matrix Splitting and Yielding | 14 |
| C. Two-Dimensional Shear-Lag Model with Broken Fibers, Longitudinal Matrix Splitting and Yielding and Transverse Matrix and Fiber Damage | 25 |
| D. Two-Dimensional Shear-Lag Model with Broken Fibers, Longitudinal Matrix Splitting and Yielding with a Surface Constraint Layer (Cover Sheet) | 31 |
| E. Two-Dimensional Shear-Lag Model with Broken Fibers, Longitudinal Matrix Splitting and Yielding with an Elastic-Linear Strain-Hardening Matrix | 37 |
| F. Two-Dimensional Shear-Lag Model with a Rectangular Notch, Longitudinal Matrix Splitting and Yielding and Transverse Matrix and Fiber Damage | 43 |
| G. Two-Dimensional Shear-Lag Model with a Circular Cut-out, Longitudinal Matrix Splitting and Yielding and Transverse Matrix and Fiber Damage | 46 |
| H. Two-Dimensional Shear-Lag Model with Broken Fibers for the Half-Plane | 50 |
| SOLUTIONS AND RESULTS | 58 |
| REFERENCES | 72 |

LIST OF FIGURES

| Figure | | Page |
|--------|--|------|
| 1. | Two-dimensional unidirectional lamina with broken fibers | 74 |
| 2. | Free-body diagram of a typical element | 75 |
| 3. | Two-dimensional unidirectional lamina with broken fibers and longitudinal matrix splitting and yielding (first quadrant) | 76 |
| 4. | Two-dimensional unidirectional lamina with broken fibers, longitudinal matrix splitting and yielding and transverse fiber and matrix damage (first quadrant) | 77 |
| 5. | Boundary conditions along the x-axis for the transverse damage model | 78 |
| 6. | Free-body diagram of an element consisting of the main lamina and the constraint layer | 79 |
| 7. | Two-dimensional unidirectional lamina with a rectangular notch, longitudinal matrix splitting and yielding and transverse damage (first quadrant) | 80 |
| 8. | Two-dimensional unidirectional lamina with a circular cut-out, longitudinal matrix splitting and yielding and transverse damage (first quadrant) | 81 |
| 9. | Free-body diagram of a typical element at the circular cut-out | 82 |
| 10. | Assembly of boundary elements for the circular cut-out | 83 |
| 11. | Two-dimensional unidirectional half-plane with broken fibers at the free edge | 84 |
| 12. | Free-body diagrams of typical elements for the half-plane problem | 85 |
| 13. | Comparison of notch tip stress distribution for seven broken fibers | 86 |

| | | |
|-----|--|----|
| 14. | Applied stress as a function of number of constrained fibers in the transverse damage zone for seven broken fibers | 87 |
| 15. | Maximum fiber stress for yielding and splitting | 88 |
| 16. | Comparison of present results (longitudinal damage model) with experimental study for a 25.4 mm by 8 ply laminate | 89 |
| 17. | Maximum fiber stress in the first intact fiber at $\eta = 0.0$, as a function of applied stress for the case of no splitting and 7 broken fibers | 90 |
| 18. | Maximum fiber stress in the first intact fiber at $\eta = 0.0$, as a function of applied stress for the case of no splitting and 29 broken fibers | 91 |
| 19. | Strength curve: Applied stress as a function of number of broken fibers | 92 |
| 20. | Comparison of notch tip stress distribution for various geometries for eleven broken fibers and no longitudinal and transverse damage | 93 |
| 21. | Comparison of notch tip stress distribution for various geometries for eleven broken fibers in the presence of longitudinal and transverse damage | 94 |

INTRODUCTION

A major portion of the writer's research over the past few years has concerned the development of suitable analytical techniques for predicting the stress state and fracture behavior of damaged composite laminates. Much of this work has dealt with approximate solutions based on discrete fiber-matrix material models with particular simplifying assumptions used to relate fiber and matrix stresses to fiber displacements. The resulting solutions are not complete solutions to the equations of elasticity for the two phase region and a significant portion of the study has been the investigation of the agreement of the results with experimental data.

In past reports and technical papers concerning this work, specific models and results have been presented in each paper, but no unified report has been written. Rather than add one more paper covering only the work of the past year it was felt to be an appropriate time in the development of these methods to review the basic assumptions and discuss the significance of the models and the results, both for the convenience of having a more complete record and to be able to make some important observations concerning the nature of the different models, about which we have only recently become aware.

The initial work in modeling a unidirectional composite containing broken fibers was presented by Hedgepeth in [1] for broken fibers with no longitudinal or transverse damage other than the initial notch. This work was extended by Hedgepeth and Van Dyke in [2] for the special case of one broken fiber with matrix yielding parallel to the fiber and

in [3] for one broken fiber with longitudinal splitting in the matrix. In all these studies the fiber breaks were assumed to lie on a transverse line and the shear-lag assumption was used. One very important feature of the shear-lag model is that it simplifies the equilibrium equations by removing the transverse displacement dependence from the longitudinal equation, and the fiber stress and the matrix shear stress can be determined without solving the transverse equation. In reference [2] Hedgepeth and Van Dyke used the same model to develop the solution for broken fibers in a three-dimensional unidirectional composite containing broken fibers with no additional damage. A detailed discussion of similar material modeling techniques and some simplified solutions are presented by Zweben in [4] and [5]. Eringen and Kim in [6] developed a modified solution for the original Hedgepeth problem, [1], by extending the shear stress-displacement relation to include fiber bending as well as axial displacements; no additional damage was accounted for in [6]. The stress-displacement relation assumed in [6] allows for better satisfaction of a stress free crack surface, i.e. the shear-lag assumption does not have sufficient freedom to remove the shear stresses from the crack surface. However, Eringen's model does couple the axial and transverse equilibrium equations and gives a somewhat more complicated set of differential-difference equations. The inclusion of matrix damage and transverse fiber breaks (notch extension) in Eringen's model appears to be much more difficult than in Hedgepeth's model and such modifications have not been attempted at this time.

The initial damage in all of the above studies consisted of broken fibers in the form of a notch (crack). Franklin in [7] and

Kulkarni et.al. in [8] investigated the case of a circular cut-out containing no additional damage and found that the stress concentrations in the unbroken fibers was changed very little over the corresponding solution for a notch.

Goree and Gross in [9] extended the Hedgepeth solutions to include longitudinal matrix yielding and splitting for an arbitrary number of broken fibers and in [10] developed a solution using the Eringen model of [6] for a three-dimensional unidirectional composite containing broken fibers but without matrix damage. The results of [9] gave very good agreement with experimental results for brittle matrix composite and reasonably good agreement for ductile matrix composites. The inclusion of transverse stable notch extension to this model is shown below to make a very significant improvement in the ability of the model to represent the behavior of a ductile matrix (boron/aluminum) laminate.

Over the past year solutions have been developed for the following problems:

1. transverse notch extension
2. constraint (or cover) layer
3. strain-hardening matrix
4. rectangular (rather than slit) initial damage region
5. circular initial damage region
6. formulation of the edge crack problem.

In the first section presented below the formulation of the original Hedgepeth problem [1] will be presented, using Fourier transform methods rather than the influence function technique as used by Hedgepeth as

this is the foundation for the remaining solutions. The next sections will then consider the development of the equations for, respectively, longitudinal splitting and yielding of the matrix, transverse notch extension, constraint layer, strain-hardening matrix, rectangular damage region, circular damage region, and the edge crack solution. Results and comparisons of the various models will then be presented.

Use of trade names or names of manufacturers in this report does not constitute an official endorsement of such products or manufacturers, either expressed or implied, by the National Aeronautics and Space Administration.

FORMULATION OF MATHEMATICAL MODELS

A. Two-Dimensional Shear-Lag Model with Broken Fibers

Consider a two-dimensional unidirectional lamina containing broken fibers as shown in Figure (1). The development presented in this section will be for no additional damage other than the broken fibers. This solution was first presented by Hedgepeth in [1]; however, as it is the fundamental solution on which all of the following models are based, it will be included in this report for completeness. Further, the method of solution appropriate for the various extensions to this basic model is somewhat different than that of Hedgepeth in [1], i.e., Fourier transform techniques are used directly in the present work while Hedgepeth developed the solution by means of influence functions. For no damage other than the initial notch the two methods are equivalent. However, for the extension to matrix yielding and splitting at the end of the notch containing more than one broken fiber, the Fourier transform method is more direct.

The formulation given below will also develop the solution for the matrix normal stress which is not given in [1]. It should be noted that it is often attributed to the shear-lag solution that only shear stresses exist in the matrix. This need not be imposed on the solution, although a fundamental property of the shear-lag assumptions is that the differential-difference equations for axial and transverse fiber displacements uncouple such that the axial displacement can be found without solving the transverse equation. As the fiber stress and matrix shear stress are functions of the axial fiber displacement alone, these stresses can then be determined without knowing the

transverse displacements. Once the axial fiber displacement is known it is a simple matter to solve the transverse equation for the transverse fiber displacement and compute the matrix normal stress between fibers.

Following Hedgepeth [1], the laminate is modeled as a two-dimensional region, shown in Figure (1), having a single row of parallel, identical, equally spaced fibers, separated by matrix. The damage is taken to consist of an arbitrary number of broken fibers such that all breaks lie along the x-axis, but they need not form a continuous break (notch). Later in this section the equations corresponding to a notch will be developed. It is this solution for a notch that is extended in the remaining sections. In all cases it is assumed that the fibers have a sufficiently higher elastic modulus in the axial direction than the matrix such that the fibers support all the axial stress in the laminate. The matrix supports transverse normal stresses and shear stresses.

Admittedly, most unidirectional composites consist of more than one lamina with all fibers in each lamina surely not perfectly aligned either through the thickness, or within each layer. These variations can have a considerable influence on the stress state. For example in [11] and [12] it is shown that the shear stress becomes larger as the fiber spacing decreases. Local failures may well occur at the critical points through the thickness in advance of laminate splitting which could give an apparent shear stiffness considerably different from that for the matrix alone. It is assumed that such variations can be accounted for by an appropriate choice of a matrix shear modulus G_M and a shear transfer distance h . It is with this in mind that the

following development will be concerned with an equivalent lamina where G_M and h are to be determined experimentally for any particular laminate. The following fundamental assumptions regarding the stress-displacement relations are made:

1. The axial fiber stress, $\sigma_F|_n$, in fiber n is given by

$$\sigma_F|_n = E_F \frac{dv_n}{dy} ,$$

where E_F is the Young's modulus of the fiber and v_n is the axial displacement of fiber n .

2. The shear stress in the matrix, $\tau|_{n+1}$, between fibers n and $n+1$ is given by

$$\tau|_{n+1} = \frac{G_M}{h} (v_{n+1} - v_n) ,$$

where G_M/h is the equivalent shear stiffness of the matrix and v_n is the axial displacement of fiber n . This relation is the basic shear-lag assumption.

3. The transverse matrix stress, $\sigma_M|_{n+1}$, between fibers n and $n+1$ is given by

$$\sigma_M|_{n+1} = \frac{E_M}{h} (u_{n+1} - u_n) ,$$

where E_M/h is the equivalent matrix transverse stiffness and u_n is the transverse displacement of fiber n .

4. Consistent with the above assumptions it then follows that the stress state on a transverse plane is constant between fibers.

With these definitions and assumptions, the equilibrium equations for a typical element as indicated in Figure (2) are as follows:

$$\frac{A_F}{t} \frac{d\sigma_F|_n}{dy} + \tau|_{n+1} - \tau|_n = 0 . \quad (A.1)$$

and

$$\sigma_M|_{n+1} - \sigma_M|_n + \frac{h}{2} \frac{d}{dy} \left\{ \tau|_{n+1} + \tau|_n \right\} = 0 \quad . \quad (\text{A.2})$$

Substituting from the above stress-displacement relations the following pair of differential-difference equations are obtained:

$$\frac{E_F A_F h}{G_M t} \frac{d^2 v_n}{dy^2} + v_{n+1} - 2v_n + v_{n-1} = 0 \quad (\text{A.3})$$

and

$$\frac{E_M}{h} \left\{ u_{n+1} - 2u_n + u_{n-1} \right\} + \frac{G_M}{h} \frac{d}{dy} \left\{ v_{n+1} - v_{n-1} \right\} = 0 \quad . \quad (\text{A.4})$$

As mentioned above, the equilibrium equation in the axial direction, equation (A.3), is seen to be independent of the transverse displacement and can be solved without solving equation (A.4). Hedgepeth [1] does not consider this transverse equation but develops a solution to the axial equation (A.3) only. We now proceed to develop a solution to equation (A.3) and, with this solution determined it will then give the solution to equation (A.4) for the transverse fiber displacements.

Noting the coefficient of the first term in equation (A.3), the following changes in the variables are suggested:

$$y = \sqrt{\frac{E_F A_F h}{G_M t}} \eta \quad , \quad (\text{A.5})$$

$$\sigma_F|_n = \sigma_\infty \bar{\sigma}_F|_n = E_F \frac{dv_n}{dy} \quad , \quad \text{and}$$

$$v_n = \sigma_\infty \sqrt{\frac{A_F h}{E_F G_M t}} V_n \quad ,$$

where η , $\bar{\sigma}_F|_n$, V_n are nondimensional. Equation (A.3) then becomes independent of all material properties as

$$\frac{d^2 V_n}{d\eta^2} + V_{n+1} - 2V_n + V_{n-1} = 0 \quad . \quad (\text{A.6})$$

This differential-difference equation can be reduced to a differential equation by defining a new function $\bar{V}(\eta, \theta)$ such that the normalized displacement $V_n(\eta)$ is the Fourier coefficient in a Fourier series expansion. That is,

$$\bar{V}(\eta, \theta) = \sum_{n=-\infty}^{\infty} V_n(\eta) e^{-in\theta} \quad , \quad \text{and} \quad (\text{A.7})$$

as the displacements are continuous functions of η , this representation is necessarily valid and can be inverted to yield

$$V_n(\eta) = \frac{1}{2\pi} \int_{-\pi}^{\pi} \bar{V}(\eta, \theta) e^{in\theta} d\theta \quad . \quad (\text{A.8})$$

Substitution for $V_n(\eta)$ in terms of $\bar{V}(\eta, \theta)$ in equation (A.6) results in

$$\frac{1}{2\pi} \int_{-\pi}^{\pi} \left\{ \frac{d^2 \bar{V}}{d\eta^2} - 2[1 - \cos(\theta)] \right\} e^{in\theta} d\theta = 0 \quad . \quad (\text{A.9})$$

This equation is of the form

$$\frac{1}{2\pi} \int_{-\pi}^{\pi} F(\eta, \theta) e^{in\theta} d\theta = 0 \quad , \quad \text{for all } \eta \quad \text{and } n.$$

The function $F(\eta, \theta)$ is continuous in θ and therefore, if the integral is to vanish for all n the function $F(\eta, \theta)$ must be zero. The equation specifying $\bar{V}(\eta, \theta)$ is then

$$\frac{d^2 \bar{V}}{d\eta^2} - \delta^2 \bar{V} = 0 \quad , \quad (\text{A.10})$$

where

$$\delta^2 = 2[1 - \cos(\theta)] = 4 \sin^2(\theta/2) \quad .$$

The solution to the problem of vanishing stresses and displacements at infinity and uniform compression on the ends of the broken fibers will now be sought. The complete solution is obtained by adding

the trivial results corresponding to uniform axial stress and no broken fibers to the following solution.

The boundary conditions are,

$$V_n(\eta) = 0 \quad \text{as } \eta \rightarrow \infty, \quad (\text{A.11})$$

for all fibers,

$$\frac{dV_n(\eta)}{d\eta} = \bar{\sigma}_F|_n = -1, \quad \text{at } \eta = 0, \quad (\text{A.12})$$

for broken fibers, and

$$V_n(\eta) = 0, \quad \text{at } \eta = 0, \quad (\text{A.13})$$

for unbroken fibers.

Equation (A.10) has the complete solution satisfying vanishing stresses and displacements remote from the damage as

$$\bar{V}(\eta, \theta) = A(\theta)e^{-\delta\eta}, \quad (\text{A.14})$$

where the function $A(\theta)$ must be determined from the remaining boundary conditions.

Using equations (A.8) and (A.14) the displacement is given by

$$V_n(\eta) = \frac{1}{2\pi} \int_{-\pi}^{\pi} A(\theta)e^{-\delta\eta} e^{in\theta} d\theta. \quad (\text{A.15})$$

Noting the form of the above integral for $\eta = 0$, the boundary condition of no displacement for the unbroken fibers, equation (A.13) is identically satisfied by taking

$$A(\theta) = \sum_{\ell} B_{\ell} e^{-i\ell\theta}, \quad (\text{A.16})$$

with ℓ being the index of each broken fiber and the B_{ℓ} are constants.

One then has precisely the number of constants B_{ℓ} as broken fibers.

These constants B_{ℓ} are determined from the remaining boundary condition, equation (A.12), of a unit compressive stress on the broken fibers at

$\eta = 0$. Substituting equation (A.16) into (A.15), equation (A.12) then gives, at $\eta = 0$,

$$\frac{1}{2\pi} \int_{-\pi}^{\pi} \sum_{\ell} B_{\ell} \delta e^{-i\ell\theta} e^{in\theta} d\theta = 1 \quad ; \quad \delta = 2 \sin(\theta/2) \quad (\text{A.17})$$

for ℓ and n corresponding to all broken fiber indices. This equation then gives a system of linear algebraic equations for the unknowns B_{ℓ} and the solution is complete. If the broken fibers are symmetric about the zero fiber, and therefore form a notch, the above equations are considerably simplified. Let the center fiber be located by the index $n=0$, then equation (A.7) may be written as a cosine series as

$$\bar{V}(\eta, \theta) = \frac{V_0(\eta)}{2} + \sum_{n=1}^{\infty} V_n(\eta) \cos(n\theta) \quad , \quad (\text{A.18})$$

from which

$$V_n(\eta) = \frac{2}{\pi} \int_0^{\pi} \bar{V}(\eta, \theta) \cos(n\theta) d\theta \quad , \quad (\text{A.19})$$

where, as in equation (A.14), $\bar{V}(\eta, \theta) = A(\theta) e^{-\delta\eta}$.

Equation (A.16) is a cosine series for this symmetric case and is given by

$$A(\theta) = \sum_{\ell=0}^N B_{\ell} \cos(\ell\theta) \quad , \quad (\text{A.20})$$

where N is the index of the last broken fiber. One then has $N+1$ unknown constants B_{ℓ} with the solution given by satisfying the boundary condition of uniform stress on the broken fibers at $\eta = 0$, equation (A.12). This gives

$$\frac{2}{\pi} \sum_{\ell=0}^N B_{\ell} \int_0^{\pi} \delta \cos(\ell\theta) \cos(n\theta) d\theta = 1 \quad , \quad n = 0, 1, \dots, N \quad (\text{A.21})$$

where, as before, recall that $\delta = 2 \sin(\theta/2)$. For example, if $N=0$

which corresponds to one broken fiber, equation (A.21) gives B_0 directly as

$$B_0 = \pi / [2 \int_0^\pi 2 \sin(\theta/2) d\theta] = \frac{\pi}{8} = A(\theta) . \quad (\text{A.22})$$

The maximum fiber stress in the first unbroken fiber is at $\eta = 0$ and is given by

$$\frac{\sigma_F|_1(0)}{\sigma_\infty} = \frac{dV_1(0)}{d\eta} = \frac{2}{\pi} \int_0^\pi -\delta A(\theta) \cos(\theta) d\theta = \frac{1}{3} ,$$

or, for a unit stress at infinity and an unloaded free end of the broken fiber

$$\bar{\sigma}_F|_1 = 1 + \frac{\sigma_F|_1(0)}{\sigma_\infty} = 1 + \frac{1}{3} = \frac{4}{3} .$$

The normalized crack opening displacement is given by equation (A.19) as

$$2V_0(0) = \frac{\pi}{2} .$$

For the general case of $2N+1$ broken fibers, and with the axial fiber displacement now known, the transverse fiber displacement $u_n(\eta)$ may be determined from equation (A.4). For the specific case of a symmetric number of broken fibers in which the axial displacement is given by an even valued transform, equation (A.19), the transverse displacement will be odd valued and is given by

$$\bar{U}(\eta, \theta) = \sum_{n=1}^{\infty} U_n(\eta) \sin(n\theta), \quad \text{and} \quad (\text{A.23})$$

$$U_n(\eta) = \frac{2}{\pi} \int_0^\pi \bar{U}(\eta, \theta) \sin(n\theta) d\theta ,$$

where

$$U_n(\eta) = \frac{u_n(\eta)}{\sigma_\infty} \sqrt{\frac{E_F G_M t}{A_F h}} . \quad (\text{A.24})$$

Substituting this representation into the normalized form of equation (A.4), the resulting transverse displacement is then given by

$$U_n(\eta) = -\frac{1}{\pi} \frac{G_M h}{E_M} \sqrt{\frac{G_M t}{A_F E_F h}} \int_0^\pi \frac{d\bar{V}(\eta, \theta)}{d\eta} \frac{\sin(\theta) \sin(n\theta)}{1 - \cos(\theta)} d\theta. \quad (\text{A.25})$$

In the following sections the above solution for a symmetric notch will be modified to account for the various damage models.

B. Two-Dimensional Shear-Lag Model with Broken Fibers and Longitudinal Matrix Splitting and Yielding

The solution developed in section A will now be extended to include longitudinal splitting and yielding of the matrix as shown in Figure (3). This solution along with extensive results is given in [9]. All the previous assumptions are assumed valid and it is only necessary to account for the additional damage region parallel to the fibers. It is assumed that splitting and yielding of the matrix initiates at the notch tip and progresses longitudinally between the last broken fiber and the first unbroken fiber as shown in Figure (3). The matrix material is assumed to be elastic-perfectly plastic.

The same free-body diagram of section A, shown in Figure (2) is considered with additional conditions for the last broken fiber, denoted by $n=N$, and $y \leq L$, to account for the longitudinal damage taken as

$$\tau \Big|_{N+1} = -\tau \langle y-\ell \rangle \quad (B.1)$$

where

$$\begin{aligned} \langle y-\ell \rangle &= 1 \quad , \quad y \geq \ell \quad , \\ \langle y-\ell \rangle &= 0 \quad , \quad y < \ell \quad , \quad \text{and} \end{aligned} \quad (B.2)$$

L equals the total damaged length, ℓ the split length, and τ_0 the matrix yield stress. Yielding is assumed to occur when the matrix shear strain reaches the yield strain, γ_0 . Splitting occurs at a multiple of γ_0 as given by the particular matrix material.

The equilibrium equations in the longitudinal and transverse directions, respectively, for all fibers n , with the exception of N and $N+1$ when $y \leq L$, are then

$$\frac{A_F}{t} \frac{d\sigma_F|_n}{dy} + \tau|_{n+1} - \tau|_n = 0 \quad , \quad (B.3)$$

and

$$\sigma_M|_{n+1} - \sigma_M|_n + \frac{h}{2} \frac{d}{dy} \left\{ \tau|_{n+1} + \tau|_n \right\} = 0 \quad . \quad (B.4)$$

For fiber N, $y \leq L$, $\tau|_{N+1} = -\tau_0 \langle y-l \rangle$, and the equilibrium equations are

$$\frac{A_F}{t} \frac{d\sigma_F|_N}{dy} - \tau_0 \langle y-l \rangle - \tau|_N = 0 \quad , \quad (B.5)$$

and

$$\sigma_M|_{N+1} - \sigma_M|_N + \frac{h}{2} \frac{d}{dy} \left\{ -\tau_0 \langle y-l \rangle + \tau|_N \right\} = 0 \quad . \quad (B.6)$$

For fiber N+1, $y \leq L$, $\tau|_{N+1} = -\tau_0 \langle y-l \rangle$, and the equilibrium equations are

$$\frac{A_F}{t} \frac{d\sigma_F|_{N+1}}{dy} + \tau|_{N+2} + \tau_0 \langle y-l \rangle = 0 \quad , \quad (B.7)$$

and

$$\sigma_M|_{N+2} - \sigma_M|_{N+1} + \frac{h}{2} \frac{d}{dy} \left\{ \tau|_{N+2} - \tau_0 \langle y-l \rangle \right\} = 0 \quad . \quad (B.8)$$

Substituting the stress-displacement relations into the equilibrium equations, the following pairs of equations are obtained:

For all fibers except N and N+1 when $y \leq L$,

$$\frac{E_F A_F h}{G_M t} \frac{d^2 v_n}{dy^2} + \left\{ v_{n+1} - 2v_n + v_{n-1} \right\} = 0 \quad , \quad (B.9)$$

and

$$\frac{E_M}{h} \left\{ u_{n+1} - 2u_n + u_{n-1} \right\} + \frac{G_M}{2} \frac{d}{dy} \left\{ v_{n+1} - v_{n-1} \right\} = 0 \quad . \quad (B.10)$$

For fiber N, $y \leq L$,

$$\frac{E_F A_F h}{G_M t} \frac{d^2 v_N}{dy^2} + v_{N-1} - v_N - \frac{h}{G_M} \tau_0 \langle y-l \rangle = 0 \quad , \quad (B.11)$$

and

$$\frac{E_M}{h} \left\{ u_{N+1} - 2u_N + u_{N-1} \right\} + \frac{h}{2} \frac{d}{dy} \left\{ \frac{G_M}{h} [v_N - v_{N-1}] - \tau_0 \langle y-l \rangle \right\} = 0. \quad (B.12)$$

For fiber N+1, $y \leq L$.

$$\frac{E_F A_F h}{G_M t} \frac{d^2 v_{N+1}}{dy^2} + v_{N+2} - v_{N+1} + \frac{h \tau_0}{G_M} \langle y-l \rangle = 0, \quad (B.13)$$

and

$$\frac{E_M}{h} \left\{ u_{N+2} - 2u_{N+1} + u_N \right\} + \frac{h}{2} \frac{d}{dy} \left\{ \frac{G_M}{h} [v_{N+2} - v_{N+1}] - \tau_0 \langle y-l \rangle \right\} = 0. \quad (B.14)$$

Again, the axial equilibrium equation is independent of the transverse displacement, u_n .

The three equilibrium equations in the longitudinal direction are then:

for all fibers, except N and N+1 when $y \leq L$,

$$\frac{E_F A_F h}{G_M t} \frac{d^2 v_n}{dy^2} + v_{n+1} - 2v_n + v_{n-1} = 0, \quad (B.15)$$

for fiber N, $y \leq L$

$$\frac{E_F A_F h}{G_M t} \frac{d^2 v_N}{dy^2} + v_{N-1} - v_N - \frac{h}{G_M} \tau_0 \langle y-l \rangle = 0, \quad (B.16)$$

and for fiber N+1, $y \leq L$

$$\frac{E_F A_F h}{G_M t} \frac{d^2 v_{N+1}}{dy^2} + v_{N+2} - v_{N+1} + \frac{h}{G_M} \tau_0 \langle y-l \rangle = 0. \quad (B.17)$$

The same change in variables as before will be used, with the following additional terms:

$$\tau_0 = \sigma_\infty \sqrt{\frac{G_M A_F}{E_F h t}} \bar{\tau}_0, \quad (B.18a)$$

$$\sigma_F|_n = \sigma_\infty \frac{dV_n}{d\eta} = \frac{\tau_0}{\bar{\tau}_0} \sqrt{\frac{E_F h t}{G_M A_F}} \frac{dV_n}{d\eta} , \quad (\text{B.18b})$$

$$\tau|_n = \sigma_\infty \sqrt{\frac{G_M A_F}{E_F h t}} \left\{ V_n - V_{n-1} \right\} = \frac{\tau_0}{\bar{\tau}_0} \left\{ V_n - V_{n-1} \right\} , \quad (\text{B.18c})$$

$$L = \sqrt{\frac{E_F A_F h}{G_M t}} \alpha \quad \text{and} \quad \ell = \sqrt{\frac{E_F A_F h}{G_M t}} \beta , \quad (\text{B.18d})$$

where η , $\bar{\sigma}_n$, V_n , $\bar{\tau}_0$, α , and β are nondimensional.

In these equations, E_F , A_F , t , L , and ℓ are taken as actual fiber modulus, fiber cross-sectional area, lamina thickness, and damage dimensions, respectively. The quantities τ_0 and G_M/h are equivalent yield stress and lamina stiffness, respectively, and are to be determined experimentally. The yield stress, τ_0 , should be reasonably close to the matrix yield stress obtained from a test using matrix material alone as long as the damage occurs in the matrix rather than along the interface or within the fiber. The quantity G_M/h is felt to be less well defined as discussed.

The resulting nondimensional equations are:

For all fibers, except N and $N+1$ when $\eta \leq \alpha$,

$$\frac{d^2 V_n}{d\eta^2} + V_{n+1} - 2V_n + V_{n-1} = 0 , \quad (\text{B.19})$$

for fiber N , $\eta \leq \alpha$

$$\frac{d^2 V_N}{d\eta^2} - V_N + V_{N-1} - \bar{\tau}_0 \langle \eta - \beta \rangle = 0 , \quad (\text{B.20})$$

and for fiber $N+1$, $\eta \leq \alpha$

$$\frac{d^2 V_{N+1}}{d\eta^2} - V_{N+1} + V_{N+2} + \bar{\tau}_0 \langle \eta - \beta \rangle = 0 . \quad (\text{B.21})$$

Defining a new unknown function $f(\eta)$ such that

$$f(\eta) = V_N - V_{N+1} - \bar{\tau}_0 \langle \eta - \beta \rangle \quad \text{if} \quad \eta < \alpha , \quad (\text{B.22})$$

and

$$f(\eta) = 0 , \quad \eta \geq \alpha$$

with $g(\eta) = V_N - V_{N+1}$ for the same range of η values, the above three equations then become:

$$\frac{d^2 V_n}{d\eta^2} + V_{n+1} - 2V_n + V_{n-1} = 0 , \quad (\text{B.23})$$

$$\frac{d^2 V_N}{d\eta^2} + V_{N+1} - 2V_N + V_{N-1} = -f(\eta) , \quad (\text{B.24})$$

and

$$\frac{d^2 V_{N+1}}{d\eta^2} + V_{N+2} - 2V_{N+1} + V_N = f(\eta) . \quad (\text{B.25})$$

These differential-difference equations may be reduced to differential equations by introducing the even valued transform as

$$\bar{V}(\eta, \theta) = \frac{V_0}{2} + \sum_{n=1}^{\infty} V_n(\eta) \cos(n\theta) , \quad (\text{B.26})$$

from which

$$V_n(\eta) = \frac{2}{\pi} \int_0^{\pi} \bar{V}(\eta, \theta) \cos(n\theta) d\theta , \quad (\text{B.27})$$

and the three equations become:

$$\frac{2}{\pi} \int_0^{\pi} \left\{ \frac{d^2 \bar{V}}{d\eta^2} - 2[1 - \cos(\theta)] \bar{V} \right\} \cos(n\theta) d\theta = 0 \quad (\text{B.28})$$

for all fibers, except N and $N+1$ when $\eta \leq \alpha$,

$$\frac{2}{\pi} \int_0^{\pi} \left\{ \frac{d^2 \bar{V}}{d\eta^2} - 2[1 - \cos(\theta)] \bar{V} \right\} \cos(n\theta) d\theta = -f(\eta) , \quad (\text{B.29})$$

fiber N, $\eta \leq \alpha$, and

$$\frac{2}{\pi} \int_0^{\pi} \left\{ \frac{d^2 \bar{V}}{d\eta^2} - 2[1 - \cos(\theta)] \bar{V} \right\} \cos(n\theta) d\theta = f(\eta) , \quad (\text{B.30})$$

fiber N+1, $\eta \leq \alpha$. Making use of the orthogonality of the circular functions these three equations may be written as one equation, valid for all values of n and η , as follows:

$$\begin{aligned} & \frac{2}{\pi} \int_0^{\pi} \left\{ \frac{d^2 \bar{V}}{d\eta^2} - 2[1 - \cos(\theta)] \bar{V} \right\} \cos(n\theta) d\theta \\ & = \frac{2}{\pi} \langle \alpha - \eta \rangle \int_0^{\pi} f(\eta) \{ \cos[(N+1)\theta] - \cos(N\theta) \} \cos(n\theta) d\theta . \end{aligned} \quad (\text{B.31})$$

This equation is of the form

$$\frac{2}{\pi} \int_0^{\pi} F(\eta, \theta) \cos(n\theta) d\theta = 0 \quad \text{for all } \eta \text{ and } n \quad (\text{B.32})$$

and noting the definition of $\bar{V}(\eta, \theta)$ in equations (B.26) and (B.27) it is seen that the function $F(\eta, \theta)$ is even valued in θ and therefore, if the integral is to vanish for all n, the function $F(\eta, \theta)$ must be zero.

The single equation specifying $\bar{V}(\eta, \theta)$ is then

$$\frac{d^2 \bar{V}}{d\eta^2} - \delta^2 \bar{V} = - \langle \alpha - \eta \rangle D^2 f(\eta) \quad (\text{B.33})$$

where

$$\delta^2 = 2[1 - \cos(\theta)] = 4 \sin^2(\theta/2) , \quad (\text{B.34})$$

and

$$D^2 = \cos(N\theta) - \cos[(N+1)\theta] . \quad (\text{B.35})$$

It is very significant that the irregular boundary condition, equation (B.1), of specified stress over a finite length, not coincident

with either coordinate axis can be accounted for exactly and that the problem reduces to one differential equation which must satisfy boundary conditions along the coordinate axes only. The ability to do so strongly depends on the form of the failure criterion. A condition in which both normal and shear stresses were included generally would couple the axial and transverse equilibrium equations and yield a far more complicated set of differential equations.

The solution to the problem of vanishing stresses and displacements at infinity and uniform compression on the ends of the broken fibers will now be sought. The complete solution is obtained by adding the results corresponding to uniform axial stress and no broken fibers to the following solution.

The boundary conditions are then

$$V_n = 0 \quad \text{as } \eta \rightarrow \infty, \quad (\text{B.36})$$

for all fibers,

$$\frac{dV_n}{d\eta} = \bar{\sigma}_F|_n = -1, \quad \text{for } \eta = 0, \quad (\text{B.37})$$

for broken fibers, and

$$V_n = 0, \quad \text{for } \eta = 0, \quad (\text{B.38})$$

for unbroken fibers.

Using a technique such as variation of parameters to determine a particular solution to equation (B.33), the complete solution satisfying stresses and displacements at infinity is

$$\bar{V}(\eta, \theta) = A(\theta)e^{-\delta\eta} + \frac{D^2}{\delta} \int_n^{\alpha-\eta} \sinh[\delta(\eta-t)]f(t)dt \quad (\text{B.39})$$

where the unknown functions are $A(\theta)$ and $f(t)$. The remaining two boundary conditions give

$$\frac{dV_n(0)}{d\eta} = \frac{2}{\pi} \int_0^\pi \left\{ -\delta A(\theta) + D^2 \int_0^\alpha \cosh(\delta t) f(t) dt \right\} \cos(n\theta) d\theta = -1 \quad (\text{B.40})$$

for all broken fibers, and

$$V_n(0) = \frac{2}{\pi} \int_0^\pi \left\{ A(\theta) - \frac{D^2}{\delta} \int_0^\alpha \sinh(\delta t) f(t) dt \right\} \cos(n\theta) d\theta = 0 \quad (\text{B.41})$$

for all unbroken fibers. Equation (B.41) is solved exactly by taking

$$A(\theta) - \frac{D^2}{\delta} \int_0^\alpha \sinh(\delta t) f(t) dt = \sum_{m=0}^N B_m \cos(m\theta) \quad (\text{B.42})$$

where the B_m are constants. Equation (B.40) then gives a system of $N+1$ algebraic equations for the $N+1$ constants B_m in terms of $f(\eta)$ which is, as yet, unknown. For the case of no damage the problem is then exactly the same as section A of the present report.

For matrix damage, $\alpha \neq 0$, equation (B.40) must be supplemented by the condition that

$$\begin{aligned} f(\eta) &= g(\eta) - \bar{\tau}_0 \langle \eta - \beta \rangle, \quad \eta \leq \alpha \\ &= V_N - V_{N+1} - \bar{\tau}_0 \langle \eta - \beta \rangle, \end{aligned} \quad (\text{B.43})$$

and recall from equation (B.22) that $f(\alpha) = 0$ and therefore

$$g(\alpha) = \bar{\tau}_0. \quad (\text{B.44})$$

The constants B_m and the function $g(\eta)$ are then specified by requiring that equations (B.40), (B.43) and (B.44) be satisfied. Using equation (B.39) and after considerable algebraic manipulation, the displacement of any fiber for all values of η is

$$\begin{aligned} V_n &= \frac{2}{\pi} \int_0^\pi e^{-\delta \eta} \sum_{m=0}^N \cos(m\theta) \cos(n\theta) d\theta \\ &\quad + \frac{1}{2} \int_0^\alpha f(t) \{C_n(|t-\eta|) - C_n(t+\eta)\} dt, \end{aligned} \quad (\text{B.45})$$

where

$$C_n(\xi) = \frac{2}{\pi} \int_0^\pi \frac{D^2}{\delta} e^{-\delta\xi} \cos(n\theta) d\theta$$

Equation (B.40) then becomes

$$\begin{aligned} \frac{2}{\pi} \int_0^\pi \left\{ -\delta \sum_{m=0}^N B_m \cos(m\theta) + D^2 \int_0^\alpha e^{-\delta t} g(t) dt - D^2 \bar{\tau}_0 \int_\beta^\alpha e^{-\delta t} dt \right\} \\ \times \cos(n\theta) d\theta = -1, \quad n=0,1,\dots,N \end{aligned} \quad (B.46)$$

and equation (B.43) along with (B.45) gives, for $n \leq \alpha$,

$$\begin{aligned} g(n) &= V_N - V_{N+1}, \\ &= \frac{2}{\pi} \int_0^\pi e^{-\delta n} \sum_{m=0}^N B_m \cos(m\theta) \{ \cos(N\theta) - \cos[(N+1)\theta] \} d\theta \\ &\quad + \frac{1}{2} \int_0^\alpha g(t) \left\{ C_N(|t-n|) - C_N(t+n) - C_{N+1}(|t-n|) + C_{N+1}(t+n) \right\} dt \\ &\quad - \frac{\bar{\tau}_0}{2} \int_\beta^\alpha \left\{ C_N(|t-n|) - C_N(t+n) - C_{N+1}(|t-n|) + C_{N+1}(t+n) \right\} dt. \end{aligned} \quad (B.47)$$

The condition that

$$g(\alpha) = \bar{\tau}_0 \quad (B.48)$$

also must be satisfied.

Physically, it would be more direct to specify the applied stress σ_∞ and the number of broken fibers, N , and determine the damage zone α and β depending on given yielding and splitting conditions. As α and β appear in the limits of the above integrals this is not convenient mathematically and it is easier to specify the number of broken fibers, N , and the damage zone α and β , and compute the required applied stress σ_∞ .

These equations were solved as follows:

(I) An initial set of constants B_m was determined for the problem of no damage, $\alpha = \beta = 0$ in equation (B.46), i.e.,

$$\sum_{m=0}^N B_m \frac{2}{\pi} \int_0^{\pi} \delta \cos(m\theta) \cos(n\theta) d\theta = 1, \quad n = 0, 1, \dots, N. \quad (B.49)$$

(II) These initial constants were then substituted into the integral equation (B.47) and, along with equation (B.48), the function $g(\eta)$ and $\bar{\tau}_0$ were determined using the desired values for α and β .

(III) Using $g(\eta)$ and $\bar{\tau}_0$, a new set of constants, B_m , was computed from equation (B.46) with the desired values of α and β .

(IV) This procedure was repeated until the unknowns changed less than a prescribed amount with additional iterations.

In the above solution the unknown function, $g(\eta)$, was assumed to be piecewise linear over the interval $0 \leq \eta \leq \alpha$ of the form

$$g^i(\eta) = \gamma_0^i + \gamma_1^i \eta, \quad i = 1, 2, \dots, k$$

when the interval was divided into k equal subdivisions. The function $g(\eta)$ then contained $2k$ unknowns with one additional unknown being $\bar{\tau}_0$. As $g(\eta)$ is the displacement difference it should be a positive, monotonically decreasing function and its representation as a piecewise linear function should be sufficiently accurate. The $(k+1)$ equations were obtained by requiring that the integral equation, equation (B.47), be satisfied at the $(k+1)$ end points, $(k-1)$ equations resulted from the requirement of continuity of the function $g(\eta)$ between adjacent intervals and the last equation was given by $g(\alpha) = \bar{\tau}_0$.

With the longitudinal displacement v_η now known, the transverse displacement u_η is obtained by solving equations (B.4), (B.6), and (B.8). This solution is recorded below for completeness.

$$u_n = - \frac{\sigma_\infty G_M h}{\pi E_M E_F} \int_0^\pi \left\langle \sin(\theta) \frac{d\bar{v}}{d\eta} - \frac{1}{2} \frac{df}{d\eta} \{ \sin(N\theta) + \sin[(N+1)\theta] \} \right\rangle \frac{\sin(n\theta) d\theta}{1 - \cos(\theta)} . \quad (\text{B.50})$$

The matrix normal stress, $\sigma_M|_n$, is related to the transverse displacement, u_n , through the stress-displacement relations discussed in section A. Knowing u_n from equation (B.50) the matrix normal stress can be computed for all values of n and η .

In the next section this solution is modified to account for transverse damage.

C. Two-Dimensional Shear-Lag Model with Broken Fibers, Longitudinal Matrix Splitting and Yielding and Transverse Matrix and Fiber Damage

A certain amount of stable transverse extension of the initial notch under increasing applied loads has been observed in tests on unidirectional and cross-ply composite laminates [13]. In case of single-ply and multi-ply unidirectional laminate this occurs in the form of breakage of an arbitrary number of fibers ahead of the initial notch tip sometimes accompanied by fracturing of the matrix and more often without any matrix fracture. In the later case the damage may be observed with x-ray or by etching away the matrix. The matrix material undergoes extensive longitudinal yielding in both the cases. This behavior appears to be strongly dependent on the laminate thickness; a detailed investigation into this question is currently underway by the present writers. The breakage of fibers is found to not be confined to a straight line in the transverse direction, that is, all fibers do not break along the x-axis even though the initial notch is oriented along the x-axis. This creates a zone ahead of the notch tip in which fibers do not possess their original stiffness and hence results in a reduced axial load carrying capacity of these fibers. If all the fiber breaks are not along the same line this reduction will not be as drastic as for rectilinear extension and thus the damage zone will support considerably more load than that of a matrix region alone.

In order to account for this behavior, an idealized model having transverse damage ahead of the initial notch in addition to the longitudinal matrix damage considered in section B is now developed.

This is shown in Figure (4). It is mathematically untractable to account for the distribution of breakage of fibers occurring at points other than those on the x-axis; the model then assumes all breaks to occur on the x-axis and accounts for the stiffness by assuming these fibers to carry a reduced load as described below. The transverse damage consists of an arbitrary number of broken fibers which are constrained by the adjoining matrix and/or by the unbroken fibers through the thickness. These fibers in the transverse damage zone will be referred to as constrained fibers. The extent of constraint is represented by a stiffness coefficient γ and is assumed to be constant for all the constrained fibers. The stiffness coefficient, γ , is given by

$$\gamma = \frac{\text{stress in the constrained fiber}}{\text{stress in the first unbroken fiber}} \cdot$$

Longitudinal damage, yielding and splitting, is assumed to occur at the end of the original notch as in section A.

With reference to Figure (4), $n = 0, 1, \dots, N$ corresponds to broken fibers in the initial notch region, $n = N + 1, N + 2, \dots, M$ corresponds to constrained fibers in the transverse damage zone and $n = M + 1, M + 2, \dots, \infty$ corresponds to unbroken fibers. By comparing Figures (2) and (4), it may be observed that the only difference between this model and the one considered in section B is in the boundary conditions along the x-axis. These boundary conditions are given in Figure (5). The governing differential-difference equations and also the final equation specifying $\bar{V}(\eta, \theta)$ will be the same as those of section B. Starting from the differential equation derived in section B, the solution is obtained using the appropriate boundary conditions following the procedure described in section B.

The governing differential equation is given by

$$\frac{d^2\bar{V}}{d\eta^2} - \delta^2\bar{V} = - \langle \alpha - \beta \rangle D^2 f(\eta) \quad , \quad (C.1)$$

where all the quantities have the same meaning as in section B. With reference to Figure (5), the boundary conditions, after normalization are given as follows:

$$(i) \quad \text{As } \eta \rightarrow \infty \quad V_n = 0 \quad \text{for all fibers.} \quad (C.2)$$

$$(ii) \quad \text{At } \eta = 0 \quad \frac{dV_n}{d\eta} = \bar{\sigma}_F|_n = -1 \quad \text{for broken fibers,} \quad (C.3)$$

and

$$\frac{dV_n}{d\eta} = \bar{\sigma}_F|_n = -1 + \gamma \bar{\sigma}_F|_{M+1} \quad \text{for broken fibers,} \quad (C.4)$$

where $\bar{\sigma}_F|_{M+1}$ is the normalized stress in the first unbroken fiber at $\eta = 0$ and γ is the stiffness coefficient defined earlier.

$$(iii) \quad \text{At } \eta = 0 \quad V_n = 0 \quad \text{for unbroken fibers.} \quad (C.5)$$

As in section B, the complete solution to equation (C.1) satisfying vanishing stresses and displacements at infinity is given by

$$\bar{V}(\eta, \theta) = A(\theta)e^{-\delta\eta} + \frac{D^2}{\delta} \langle \alpha - \beta \rangle \int_0^\alpha \sinh[\delta(\eta-t)] f(t) dt \quad , \quad (C.6)$$

where the unknown functions are $A(\theta)$ and $f(t)$. The remaining two boundary conditions give

$$\frac{dV_n(0)}{d\eta} = \frac{2}{\pi} \int_0^\pi \left\{ -\delta A(\theta) + D^2 \int_0^\alpha \cosh(\delta t) f(t) dt \right\} \cos(n\theta) d\theta = -1 \quad n = N+1, \dots, N, \quad (C.7)$$

$$\frac{dV_n(0)}{d\eta} = \frac{2}{\pi} \int_0^\pi \left\{ -\delta A(\theta) + D^2 \int_0^\alpha \cosh(\delta t) f(t) dt \right\} \cos(n\theta) d\theta = -1 + \gamma \bar{\sigma}_F|_{M+1} \quad n = N+1, \dots, M, \quad (C.8)$$

and

$$V_n(0) = \frac{2}{\pi} \int_0^\pi \left\{ A(\theta) - \frac{D^2}{\delta} \int_0^\alpha \sinh(\delta t) f(t) \right\} \cos(n\theta) d\theta = 0$$

$$n = M+1, M+2, \dots, \infty. \quad (C.9)$$

Equation (C.9) is solved exactly by taking

$$A(\theta) - \frac{D^2}{\delta} \int_0^\alpha \sinh(\delta t) f(t) dt = \sum_{m=0}^M B_m \cos(m\theta) \quad (C.10)$$

where B_m are constants. The stress in the first intact fiber,

$\bar{\sigma}_F|_{M+1}$, is given by

$$\frac{dV_{M+1}(0)}{dn} = \frac{2}{\pi} \int_0^\pi \left\{ -\delta A(\theta) + D^2 \int_0^\alpha \cosh(\delta t) f(t) dt \right\} \cos[(M+1)\theta]$$

$$= -1 + \bar{\sigma}_F|_{M+1}. \quad (C.11)$$

Using equations (C.10) and (C.11) in equations (C.7) and (C.8), $A(\theta)$

and $\bar{\sigma}_F|_{M+1}$ may be eliminated resulting in $M+1$ algebraic equations for

$M+1$ constants B_m in terms of $f(\eta)$ which is, as yet, unknown. For

longitudinal matrix damage, equations (C.7) and (C.8) must be supple-

mented by the conditions that

$$f(\eta) = g(\eta) - \bar{\tau}_0 \langle \eta - \beta \rangle, \quad \eta < \alpha, \quad (C.12)$$

and

$$g(\alpha) = \bar{\tau}_0. \quad (C.13)$$

From equations (C.6) and (C.10), $A(\theta)$ may be eliminated to obtain

$\bar{V}(\eta, \theta)$ in terms of constants B_m and unknown function $f(t)$. Recalling

the relation between $\bar{V}(\eta, \theta)$ and $V_n(\eta)$, an expression can be obtained

for the axial fiber displacement $V_n(\eta)$ as

$$V_n(\eta) = \frac{2}{\pi} \int_0^\pi e^{-\delta\eta} \sum_{m=0}^M B_m \cos(m\theta) \cos(n\theta) d\theta$$

$$+ \frac{1}{2} \int_0^\alpha f(t) \{C_n(|t-\eta|) - C_n(t+\eta)\} dt, \quad (C.14)$$

where

$$C_n(\xi) = \frac{2}{\pi} \int_0^\pi \frac{D^2}{\delta} e^{-\delta\xi} \cos(n\theta) d\theta \quad . \quad (C.15)$$

Equations (C.7) and (C.8) then become

$$\frac{2}{\pi} \int_0^\pi \left\{ -\delta \sum_{m=0}^M B_m \cos(m\theta) + D^2 \int_0^\alpha e^{-\delta t} g(t) dt - D^2 \bar{\tau}_0 \int_\beta^\alpha e^{-\delta t} dt \right\} \times \cos(n\theta) d\theta = -1 \quad n = 0, 1, \dots, N, \quad (C.16)$$

and

$$\frac{2}{\pi} \int_0^\pi \left[-\delta \sum_{m=0}^M B_m \cos(m\theta) + D^2 \int_0^\alpha e^{-\delta t} g(t) dt - \bar{\tau}_0 D^2 \int_\beta^\alpha e^{-\delta t} dt \right] \times \{\cos(n\theta) - \gamma \cos[(M+1)\theta]\} d\theta = -1 + \gamma \quad n = N+1, \dots, M. \quad (C.17)$$

Equation (C.12) along with equation (C.14) gives

$$g(\eta) = \frac{2}{\pi} \int_0^\pi e^{-\delta\eta} \sum_{m=0}^M B_m \cos(m\theta) \{\cos(n\theta) - \cos[(N+1)\theta]\} d\theta + \frac{1}{2} \int_0^\alpha g(t) \left\{ C_N(|t-\eta|) - C_N(t+\eta) - C_{N+1}(|t-\eta|) + C_{N+1}(t+\eta) \right\} dt - \frac{\bar{\tau}_0}{2} \int_\beta^\alpha \left\{ C_N(|t-\eta|) - C_N(t+\eta) - C_{N+1}(|t-\eta|) + C_{N+1}(t+\eta) \right\} dt. \quad (C.18)$$

The condition that

$$g(\alpha) = \bar{\tau}_0 \quad (C.19)$$

must also be satisfied.

Equations (C.16) to (C.19) are of the same form as those obtained in section B for $g(\eta)$ and the constants B_m ; however, they now contain the additional parameters M and γ . The procedure to obtain displacements and stresses is the same as before. For boron/aluminum laminate the size of the damage zone ($M-N$) was found to be approximately constant for all initial notch lengths (N). The coefficient γ decreased with an

increase in the initial notch length. The results are discussed below where it is shown that stable transverse notch extension is possible, with the extension becoming unstable in a boron/aluminum laminate at about seven damaged fibers.

D. Two-Dimensional Shear-Lag Model with Broken Fibers, Longitudinal Matrix Splitting and Yielding with a Surface Constraint Layer (Cover Sheet)

A constraint layer is added parallel to the main lamina of the problem considered in Section B, providing additional shear stiffness. The constraint layer is an attempt to account for either the misalignment of fibers in a multi-ply unidirectional laminate, or the presence of a non-zero ply in the composite laminate. The extent of the above effects may be represented by the amount of constraint the layer introduces, defined in Figure (6) as the constraint ratio. The constraint ratio may be varied by varying the constraint layer parameters. However, in the present investigation no explicit relationship between the constraint ratio and constraint layer parameters is considered. Displacement-stress relations similar to those in section B are assumed so as to obtain decoupling of the equilibrium equations. Only fiber stresses and matrix shear stresses will be developed in the present study. The equilibrium equations in the transverse direction are more difficult than those in the previous models due to the presence of the constraint layer and will be considered at a later time.

A free-body diagram of an element consisting of the main lamina and the constraint layer is shown in Figure (6). With reference to the free-body diagram, the equilibrium equations in the axial directions are given below. For all fibers n , with the exception of N and $N+1$ when $y \leq L$ the equilibrium equation is

$$\frac{A_F}{t} \frac{d\sigma_F|_n}{dy} + \tau|_{n+1} - \tau|_n = 0 . \quad (D.1)$$

For fiber N and $N+1$, $y \leq L$, $\tau|_{N+1} = -\tau_0 \langle y-L \rangle$ and the equilibrium equations are

$$\frac{A_F}{t} \frac{d\sigma_F|_N}{dy} - \tau_0 \langle y-l \rangle - \tau|_N + \left\{ \tau'|_{N+1} - \tau'|_N \right\} \frac{t'}{t} = 0, \quad (D.2)$$

and

$$\frac{A_F}{t} \frac{d\sigma_F|_{N+1}}{dy} + \tau|_{N+2} + \tau_0 \langle y-l \rangle + \left\{ \tau'|_{N+2} - \tau'|_{N+1} \right\} \frac{t'}{t} = 0. \quad (D.3)$$

The following stress-displacement relations are introduced in equations (D.1) through (D.3) as before:

$$\begin{aligned} \sigma_F|_n &= E_F \frac{dv_n}{dy}, \\ \tau|_{n+1} &= \frac{G_M}{h} (v_{n+1} - v_n), \quad \text{and} \\ \tau'|_{n+1} &= \frac{G'}{h'} (v_{n+1} - v_n). \end{aligned} \quad (D.4)$$

The equations (D.1) through (D.3) then become

$$\frac{A_F E_F}{t} \frac{d^2 v_n}{dy^2} + \frac{G_M}{h} (v_{n+1} - 2v_n + v_{n-1}) + \frac{G' t'}{h' t} (v_{n+1} - 2v_n + v_{n-1}) = 0 \quad (D.5)$$

for all fibers, except N and N+1 when $y \leq L$,

$$\frac{A_F E_F}{t} \frac{d^2 v_N}{dy^2} - \tau_0 \langle y-l \rangle - \frac{G_M}{h} (v_N - v_{N-1}) + \frac{G' t'}{h' t} (v_{N+1} - 2v_N + v_{N-1}) = 0 \quad (D.6)$$

for fiber N when $y \leq L$, and

$$\frac{A_F E_F}{t} \frac{d^2 v_{N+1}}{dy^2} + \tau_0 \langle y-l \rangle + \frac{G_M}{h} (v_{N+2} - v_{N+1}) + \frac{G' t'}{h' t} (v_{N+2} - 2v_{N+1} + v_N) = 0 \quad (D.7)$$

for fiber N+1 when $y \leq L$.

By defining $C_R = \frac{G'}{h'} \frac{t'}{t} \frac{h}{G_M}$ = constraint ratio, and rearranging terms, equations (D.5) through (D.7) may be rewritten as

$$\frac{A_F E_F h}{G_M t} \frac{d^2 v_n}{dy^2} + (1 + C_R)(v_{n+1} - 2v_n + v_{n-1}) = 0 \quad , \quad (D.8)$$

$$\frac{A_F E_F h}{G_M t} \frac{d^2 v_N}{dy^2} + (1 + C_R)(v_{N+1} - 2v_N + v_{N-1}) = \frac{h}{G_M} \tau_0 \langle y-\ell \rangle + v_{N+1} - v_N \quad , \quad (D.9)$$

and

$$\frac{A_F E_F h}{G_M t} \frac{d^2 v_{N+1}}{dy^2} + (1 + C_R)(v_{N+2} - 2v_{N+1} + v_N) = v_N - v_{N+1} - \frac{h}{G_M} \tau_0 \langle y-\ell \rangle \quad . \quad (D.10)$$

The same change of variables as in Section B will be used in order to normalize the quantities in the equilibrium equations. The resulting nondimensional equilibrium equations are:

for all fibers, except N and N+1 when $\eta \leq \alpha$,

$$\frac{d^2 V_n}{d\eta^2} + (1 + C_R)(V_{n+1} - 2V_n + V_{n-1}) = 0 \quad , \quad (D.11)$$

for fiber N, when $\eta \leq \alpha$

$$\frac{d^2 V_N}{d\eta^2} + (1 + C_R)(V_{N+1} - 2V_N + V_{N-1}) = V_{N+1} - V_N + \bar{\tau}_0 \langle \eta-\beta \rangle \quad , \quad (D.12)$$

and for fiber N+1, $\eta \leq \alpha$

$$\frac{d^2 V_{N+1}}{d\eta^2} + (1 + C_R)(V_{N+2} - 2V_{N+1} + V_N) = - (V_{N+1} - V_N) - \bar{\tau}_0 \langle \eta-\beta \rangle \quad . \quad (D.13)$$

Defining a new function $f(\eta)$ such that

$$f(\eta) = V_N - V_{N+1} - \bar{\tau}_0 \langle \eta-\beta \rangle \quad \text{if} \quad \eta < \alpha \quad , \quad (D.14)$$

$$\text{and} \quad f(\eta) = 0 \quad \text{if} \quad \eta \geq \alpha \quad , \quad (D.15)$$

with $g(\eta) = V_N - V_{N+1}$, for the same range of η values, the above three equations then become:

$$\frac{d^2 V_n}{dn^2} + (1 + C_R)(V_{n+1} - 2V_n + V_{n-1}) = 0 , \quad (D.16)$$

$$\frac{d^2 V_N}{dn^2} + (1 + C_R)(V_{N+1} - 2V_N + V_{N-1}) = - f(n), \quad (D.17)$$

and

$$\frac{d^2 V_{N+1}}{dn^2} + (1 + C_R)(V_{N+2} - 2V_{N+1} + V_N) = f(n). \quad (D.18)$$

These differential-difference equations may be reduced to differential equations by introducing a new function $\bar{V}(n, \theta)$ previously defined in section B, so that, $V_n(n)$ is given by

$$V_n(n) = \frac{2}{\pi} \int_0^\pi \bar{V}(n, \theta) \cos(n\theta) d\theta . \quad (D.19)$$

After substituting for $V_n(n)$ from equation (D.19) the above three equations become, respectively,

$$\frac{2}{\pi} \int_0^\pi \left\{ \frac{d^2 \bar{V}}{dn^2} - 2(1 + C_R)[1 - \cos(\theta)] \bar{V} \right\} \cos(n\theta) d\theta = 0 , \quad (D.20)$$

$$\frac{2}{\pi} \int_0^\pi \left\{ \frac{d^2 \bar{V}}{dn^2} - 2(1 + C_R)[1 - \cos(\theta)] \bar{V} \right\} \cos(N\theta) d\theta = - f(n) , \quad (D.21)$$

and

$$\frac{2}{\pi} \int_0^\pi \left\{ \frac{d^2 \bar{V}}{dn^2} - 2(1 + C_R)[1 - \cos(\theta)] \bar{V} \right\} \cos[(N+1)\theta] d\theta = f(n) . \quad (D.22)$$

Making use of the orthogonality of the circular functions these three equations may be written as one equation, valid for all values of n and n as follows:

$$\begin{aligned} & \frac{2}{\pi} \int_0^\pi \left\{ \frac{d^2 \bar{V}}{dn^2} - 2(1 + C_R)[1 - \cos(\theta)] \bar{V} \right\} \cos(n\theta) d\theta \\ & = \frac{2}{\pi} \langle \alpha - n \rangle \int_0^\pi f(n) \{ \cos[(N+1)\theta] - \cos(N\theta) \} \cos(n\theta) d\theta . \end{aligned} \quad (D.23)$$

This equation is of the form

$$\frac{2}{\pi} \int_0^{\pi} F(\eta, \theta) \cos(n\theta) d\theta = 0 \quad , \quad \text{for all } \eta \text{ and } n \quad .$$

Since $F(\eta, \theta)$ is even valued in θ , if the integral is to vanish for all n the function, $F(\eta, \theta)$, must be zero. The single equation specifying $\bar{V}(\eta, \theta)$ is then given by

$$\frac{d^2 \bar{V}}{d\eta^2} - \delta^2 \bar{V} = -\langle \alpha - \eta \rangle D^2 f(\eta) \quad , \quad (D.24)$$

$$\delta^2 = 2(1 + C_R)[1 - \cos(\theta)] = [2\sqrt{1 + C_R} \sin(\theta/2)]^2 \quad , \quad (D.25)$$

and

$$D^2 = \cos(N\theta) - \cos[(N+1)\theta] \quad . \quad (D.26)$$

The equation (D.24) is exactly of the same form as the corresponding differential equation, equation (B.33) of section B, the only difference being in the definition of δ . Consequently, the expression for $V_n(\eta)$, the algebraic equations for the constant B_m , and the integral equation are the same as in section B. They are reproduced here for completeness.

The displacement of any fiber for all values of η is

$$V_n(\eta) = \frac{2}{\pi} \int_0^{\pi} e^{-\delta\eta} \sum_{m=0}^N B_m \cos(m\theta) \cos(n\theta) d\theta \\ + \frac{1}{2} \int_0^{\alpha} f(t) \left\{ C_n(|t-\eta|) - C_n(t+\eta) \right\} dt \quad , \quad (D.27)$$

where

$$C_n(\zeta) = \frac{2}{\pi} \int_0^{\pi} \frac{D^2}{\delta} e^{-\delta\zeta} \cos(n\theta) d\theta \quad .$$

The algebraic equations for the constants B_m are given by

$$\frac{2}{\pi} \int_0^{\pi} \left\{ -\delta \sum_{m=0}^N B_m \cos(m\theta) + D^2 \int_0^{\alpha} e^{-\delta t} g(t) dt - D^2 \bar{\tau}_0 \int_{\beta}^{\alpha} e^{-\delta t} dt \right\} \times \cos(n\theta) dt = -1, \quad n = 0, 1, \dots, N. \quad (D.28)$$

The function $g(n)$ is given by the integral equation

$$g(n) = \frac{2}{\pi} \int_0^{\pi} e^{-\delta n} \sum B_m \cos(m\theta) D^2 d\theta + \frac{1}{2} \int_0^{\alpha} g(t) \left\{ C_N(|t-n|) - C_N(t+n) - C_{N+1}(|t-n|) + C_{N+1}(t+n) \right\} dt - \frac{\bar{\tau}_0}{2} \int_{\beta}^{\alpha} \left\{ C_N(|t-n|) - C_N(t+n) - C_{N+1}(|t-n|) + C_{N+1}(t+n) \right\} dt. \quad (D.29)$$

The condition that

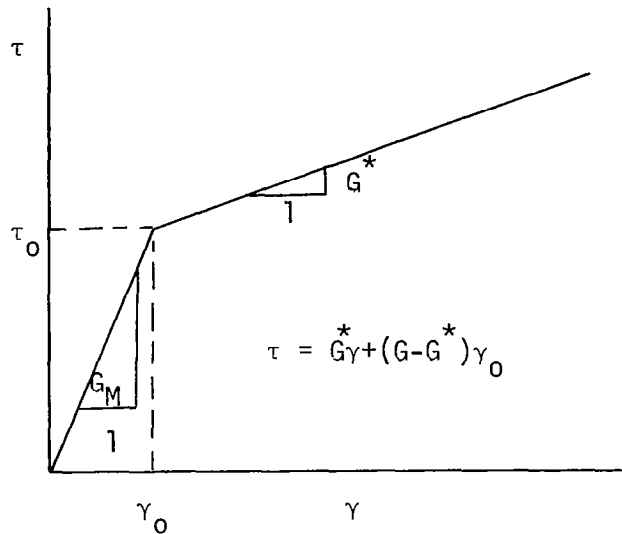
$$g(\alpha) = \bar{\tau}_0,$$

must also be satisfied.

The numerical technique described in section B is employed to obtain the solution to the above equations.

E. Two-Dimensional Shear-Lag Model with Broken Fibers, Longitudinal Matrix Splitting, and Yielding with an Elastic-Linear Strain-Hardening Matrix

In section B, longitudinal matrix splitting and yielding was considered with the matrix material being elastic-perfectly plastic. In this section a bilinear stress-strain behavior for the matrix material is assumed, as shown in the figure below.



Bilinear stress-strain relationship

A free-body diagram for a typical element is given in Figure (2) with the special condition for the last broken fiber, N now given by

$$\tau|_{N+1} = [G^*\gamma_{N+1} - (G_M - G^*)\gamma_0] \langle y - \ell \rangle, \quad (E.1)$$

where the negative sign is taken to account for negative shear strain, so that the absolute value of γ_0 is specified.

The equilibrium equations in the longitudinal and transverse directions, respectively, for all fibers n, with the exception of N and N+1 when $y \leq L$ are

$$\frac{A_F}{t} \frac{d\sigma_F|_n}{dy} + \tau|_{n+1} + \tau|_n = 0 ,$$

and

$$\sigma_M|_{n+1} - \sigma_M|_n + \frac{h}{2} \frac{d}{dy} (\tau|_{n+1} + \tau|_n) = 0 . \quad (E.2)$$

For fiber N, $y \leq L$ the equilibrium equations are

$$\frac{A_F}{t} \frac{d\sigma_F|_N}{dy} + [G^*\gamma_{N+1} - (G_M - G^*)\gamma_0] \langle y-l \rangle - \tau|_N = 0 ,$$

and

$$\sigma_M|_{N+1} - \sigma_M|_N + \frac{h}{2} \frac{d}{dy} [G^*\gamma_{N+1} - (G_M - G^*)\gamma_0] \langle y-l \rangle + \tau|_N = 0 . \quad (E.3)$$

For fiber N+1, $y \leq L$ the equilibrium equations are

$$\frac{A_F}{t} \frac{d\sigma_F|_{N+1}}{dy} + \tau|_{N+2} - [G^*\gamma_{N+1} - (G_M - G^*)\gamma_0] \langle y-l \rangle = 0 ,$$

and

$$\sigma_M|_{N+2} - \sigma_M|_{N+1} + \frac{h}{2} \frac{d}{dy} [\tau|_{N+2} + \{G^*\gamma_{N+1} - (G_M - G^*)\gamma_0\} \langle y-l \rangle] = 0 . \quad (E.4)$$

Introducing the stress-displacement relations defined in sections A and B, and also noting that $\gamma_{n+1} = (v_{n+1} - v_n)/h$, the equilibrium equations in the longitudinal direction may be written as follows.

For all fibers except N and N+1 when $y \leq L$,

$$\frac{A_F E_F h}{G_M t} \frac{d^2 v_n}{dy^2} + (v_{n+1} - 2v_n + v_{n-1}) = 0 . \quad (E.5)$$

For fiber N, when $y \leq L$,

$$\begin{aligned} \frac{A_F E_F h}{G_M t} \frac{d^2 v_N}{dy^2} + (v_{N-1} - v_N) - (1 - \frac{G^*}{G_M}) \frac{h}{G_M} \tau_0 \langle y-l \rangle \\ + \frac{G^*}{G_M} (v_{N+1} - v_N) \langle y-l \rangle = 0 . \end{aligned} \quad (E.6)$$

For fiber N+1, when $y \leq L$,

$$\frac{A_F E_F h}{G_M t} \frac{d^2 v_{N+1}}{dy^2} + v_{N+2} - v_{N+1} + \left(1 - \frac{G^*}{G_M}\right) \frac{h}{G_M} \tau_0 \langle y-l \rangle - \frac{G^*}{G_M} (v_{N+1} - v_N) \langle y-l \rangle = 0. \quad (E.7)$$

The equilibrium equations in the longitudinal direction are independent of transverse displacements u_n . Therefore, only the solution for the longitudinal displacement v_n will be considered.

The same change of variables as in section B will be used in order to normalize the quantities in the equilibrium equations. The resulting nondimensional equations are:

for all fibers, except N and N+1 when $\eta \leq \alpha$

$$\frac{d^2 V_n}{d\eta^2} + V_{n+1} - 2V_n + V_{n-1} = 0, \quad (E.8)$$

for fiber N, when $\eta \leq \alpha$

$$\frac{d^2 V_N}{d\eta^2} - V_N + V_{N-1} - \left(1 - \frac{G^*}{G_M}\right) \bar{\tau}_0 \langle \eta-\beta \rangle + \frac{G^*}{G_M} (V_{N+1} - V_N) \langle \eta-\beta \rangle = 0, \quad (E.9)$$

for fiber N+1, when $\eta \leq \alpha$

$$\frac{d^2 V_{N+1}}{d\eta^2} + V_{N+2} - V_{N+1} + \left(1 - \frac{G^*}{G_M}\right) \bar{\tau}_0 \langle \eta-\beta \rangle - \frac{G^*}{G_M} (V_{N+1} - V_N) \langle \eta-\beta \rangle = 0. \quad (E.10)$$

For the sake of simplicity, let $G_R = \frac{G^*}{G_M}$ and

$$\bar{\tau}_{OR} = \left(1 - \frac{G^*}{G_M}\right) \bar{\tau}_0. \quad (E.11)$$

As before, a new function $f(\eta)$ is defined such that

$$f(\eta) = V_N - V_{N+1} - \left\{ \bar{\tau}_{OR} - G_R (V_{N+1} - V_N) \right\} \langle \eta-\beta \rangle, \text{ if } \eta < \alpha, \\ \text{and } f(\eta) = 0, \text{ if } \eta \geq \alpha. \quad (E.12)$$

With the introduction of $f(n)$, the equations (E.8) to (E.10) may be written as follows:

$$\frac{d^2 V_n}{d\eta^2} + V_{n+1} - 2V_n + V_{n-1} = 0 \quad , \quad (E.13)$$

$$\frac{d^2 V_N}{d\eta^2} + V_{N+1} - 2V_N + V_{N-1} = -f(n) \quad , \quad (E.14)$$

and

$$\frac{d^2 V_{N+1}}{d\eta^2} + V_{N+2} - 2V_{N+1} + V_N = f(n) \quad . \quad (E.15)$$

Equations (E.13) to (E.15) are exactly of the same form as the corresponding equations of section B, i.e., equations (B.23) to (B.25).

The only difference is in the function $f(n)$, which is now defined as

$$f(n) = g(n) - \bar{\tau}_{OR} \langle n-\beta \rangle \quad , \quad \text{for } \eta < \alpha \quad , \quad (E.16)$$

so that

$$g(n) = (1 - G_R \langle n-\beta \rangle)(V_N - V_{N+1}) \quad , \quad (E.17)$$

and

$$g(\alpha) = \bar{\tau}_{OR} \quad . \quad (E.18)$$

The boundary conditions on stress and displacements are the same as those of section B. Following the procedure detailed in section B, the axial displacement in fiber n for all values of η is given by

$$V_n(\eta) = \frac{2}{\pi} \int_0^\pi e^{-\delta\eta} \sum_{m=0}^N B_m \cos(m\theta) \cos(n\theta) d\theta + \frac{1}{2} \int_0^\alpha f(t) \left\{ C_n(|t-\eta|) - C_n(t+\eta) \right\} dt \quad , \quad (E.19)$$

where

$$C_n(\xi) = \frac{2}{\pi} \int_0^\pi \frac{D^2}{\delta} e^{-\delta\xi} \cos(n\theta) d\theta \quad ,$$

$$\delta = 2 \sin(\theta/2) \quad ,$$

$$\text{and } D^2 = \cos(N\theta) - \cos[(N+1)\theta] \quad .$$

Boundary conditions on fiber stress yield the following equation:

$$\frac{2}{\pi} \int_0^{\pi} \left\{ -\delta \sum_{m=0}^N B_m \cos(m\theta) + D^2 \int_0^{\alpha} e^{-\delta t} g(t) dt - D^2 \bar{\tau}_{OR} \int_{\beta}^{\alpha} e^{-\delta t} dt \right\} \times \cos(n\theta) d\theta = -1, \quad n = 0, 1, \dots, N. \quad (E.20)$$

Putting $n = N$ and $N+1$ in (E.19) and subtracting V_{N+1} from V_N gives

$$V_N - N_{N+1} = \frac{2}{\pi} \int_0^{\pi} e^{-\delta \eta} \sum_{m=0}^N B_m \cos(m\theta) D^2 d\theta + \frac{1}{2} \int_0^{\alpha} f(t) \left\{ C_N(|t-n|) - C_N(t+n) - C_{N+1}(|t-n|) + C_{N+1}(t+n) \right\} dt. \quad (E.21)$$

Multiplying equation (E.21) by $(1 - G_R \langle \eta - \beta \rangle)$ and recalling the definition of $g(\eta)$, equation (E.21) reduces to the following:

$$g(\eta) = [1 - G_R \langle \eta - \beta \rangle] \left[\frac{2}{\pi} \int_0^{\pi} e^{-\delta \eta} \sum_{m=0}^N B_m \cos(m\theta) D^2 d\theta + \frac{1}{2} \int_0^{\alpha} \left\{ g(\eta) - \bar{\tau}_{OR} \langle \eta - \beta \rangle \right\} \left\{ C_N(|t-n|) - C_N(t+n) - C_{N+1}(|t-n|) + C_{N+1}(t+n) \right\} dt \right]. \quad (E.22)$$

Further simplification of (E.22) yields the integral equation

$$g(\eta) = [1 - G_R \langle \eta - \beta \rangle] \left[\frac{2}{\pi} \int_0^{\pi} e^{-\delta \eta} \sum B_m \cos(m\theta) \cos(n\theta) D^2 d\theta + \frac{1}{2} \int_0^{\alpha} g(\eta) \left\{ C_N(|t-n|) - C_N(t+n) - C_{N+1}(|t-n|) + C_{N+1}(t+n) \right\} dt - \frac{\bar{\tau}_{OR}}{2} \int_{\beta}^{\alpha} \left\{ C_N(|t-n|) - C_N(t+n) - C_{N+1}(|t-n|) + C_{N+1}(t+n) \right\} dt \right]. \quad (E.23)$$

The last condition that must be satisfied is

$$g(\alpha) = \bar{\tau}_{OR} = \bar{\tau}_0 (1 - G_R).$$

Equations (E.20) and (E.23) together with equation (E.24) are solved employing the numerical technique described in section B in order to obtain displacements and stresses.

The above development of the different modifications to the fundamental solution of section B has been presented with each change considered separately in the past three sections (C,D and E). This procedure was used to note more clearly the necessary changes. However, in developing the computer codes for these solutions we have included all the modifications in one code and have investigated the influence of the various models as a complete set. In the results, to be discussed later in this report, it was found that the transverse damage model of section C was the most significant. The inclusion of a strain-hardening matrix had very little influence on the ability of the solution to give results consistent with experiments for ductile matrix laminates. Perhaps if unloading had been considered, more dependence would have been noted. Also, the constraint layer (cover sheet) was not significant in comparing with experimental data on unidirectional laminates, however it certainly would be for cross-ply laminates. The following two sections present the solutions for a rectangular and circular damage region without including a strain-hardening matrix or a cover layer but including all other damage. The main purpose was to investigate the changes given by different initial damage shapes.

F. Two-Dimensional Shear-Lag Model with a Rectangular Notch, Longitudinal Matrix Splitting and Yielding and Transverse Matrix and Fiber Damage

In the next two sections we extend the above solutions to account for an initial damage zone in the shape of respectively; a rectangular notch and a circular cut-out. These represent more realistic damage shapes and it is of primary interest to investigate the differences in the results as compared to the idealized model of a slit as previously discussed. The same basic assumptions as before will be made and, as the solutions are developed very easily from the past work, only the fundamental differences will be discussed. Both longitudinal and transverse damage will be included initially. That is, the development will concentrate on the necessary changes to the complete solution presented in section C rather than starting with no damage and developing each successive solution. For both of these cases the only significant difference in the solutions is the change in boundary conditions on the initial damage region and, for the rectangular opening in particular, these differences give almost trivial changes in the resulting form of the equations.

The solution to be developed in this section is for an initial damage region having the form of a rectangular opening. Under loading, damage is taken, as before, in the form of longitudinal splitting and yielding of the matrix and transverse damage to the fibers. The longitudinal damage is assumed to occur at the end of the initial notch between the last broken fiber and the first unbroken fiber. Transverse damage is modeled, in the same manner as in the preceding sections, as

reduced load carrying fibers along the horizontal axis. Figure (7) depicts the geometry for this study. This last assumption is admittedly a simplification as one would assume that the location of the maximum axial stress in the first unbroken fiber in front of the notch, before transverse damage occurs, would be at the corner of the notch rather than the center. If this is true then notch extension would, at least, begin at the corner. The results from the present solution indeed indicate the maximum stress to occur at the corner. However, the difference between this maximum stress and the stress at $y=0$ is small and further, the location of the maximum stress in adjacent unbroken fibers away from the notch changes from the corner to the y -axis after only a few fibers. Preliminary experimental studies now being initiated also indicate that transverse extension does originate at the notch corners but successive breaks occur in a random manner tending to be symmetric about the x -axis. So, even though the model does not account for this irregularity in transverse extension, it is felt to be a reasonable approximation, especially for larger notch extension.

With the above assumptions, the solution is then developed by modifying the previous results to account for the boundary conditions of zero shear stress on the sides of the notch and a unit compression stress on the ends of the fiber at the top (and bottom) of the notch. As the solution already allows for matrix splitting, the first of the above conditions is met simply by setting the minimum value of the split length (β) equal to the half-notch height. The remaining boundary condition is satisfied by taking $\eta = H$ (normalized half-notch height)

rather than $\eta=0$ as in equation (B.46); this is

$$\frac{2}{\pi} \int_0^{\pi} \sum_{m=0}^N B_m \cos(m\theta) \delta e^{-\delta H} \cos(n\theta) d\theta = -1 .$$

All other equations are unchanged.

G. Two-Dimensional Shear-Lag Model with a Circular Cut-out, Longitudinal Matrix Splitting and Yielding and Transverse Matrix and Fiber Damage

The solution to this problem for the case of no additional damage was presented by Franklin in [7] and Kulkarni et. al. in [8]. Both of these studies had difficulty satisfying the stress free boundary condition of the circular boundary; Franklin's solution gave zero stress in the fibers but did not consider the non-zero shear stresses in the matrix while Kulkarni attempted to remove the shear stresses by an averaging technique. The results of the two are, however, not significantly different. In the present solution we formulate the boundary conditions in the same way as Franklin but the ability of the present model to allow for matrix splitting gives some necessary additional freedom to satisfy the stress free conditions more accurately. Longitudinal and transverse damage is also included with the longitudinal damage being at the edge of the hole and the transverse damage originating and extending along the horizontal axis as in the slit and the rectangular notch.

To develop the stress free boundary conditions on the hole surface first consider an unnotched laminate having uniform applied stresses at infinity and determine the fiber stresses on a circular region having the radius of the desired cut-out as shown in Figure (8). The negative of these stresses are then the appropriate boundary stresses to be applied to the edge of the circular hole in an infinite laminate having vanishing stresses and displacements at infinity.

A typical element on the boundary of the circular hole is shown in Figure (9). A series of these inclined elements were joined together

to form an approximation of the circular boundary as shown in Figure (10). It is seen in Figure (10) that for each element a small vertical matrix boundary exists on which the shear stress, as given by the shear-lag assumption, will not be zero. The largest such surface is between the last broken and first unbroken fiber. By setting the matrix split length (β) equal to this distance, this portion of the shear stress boundary condition is satisfied. The shear stress condition on the remaining elements is not satisfied.

Referring to Figure (9) and summing forces in the horizontal and vertical directions yields

$$A_F \sigma_\infty - t\sigma_R \ell_n \sin(\theta_n) - t\tau_{RT} \ell_n \cos(\theta_n) = 0 \quad , \quad (G.1)$$

and

$$-t\sigma_R \ell_n \cos(\theta_n) + t\tau_{RT} \ell_n \sin(\theta_n) = 0 \quad . \quad (G.2)$$

Solving for the boundary stresses yields

$$\sigma_R = \sigma_\infty \frac{A_F}{h\bar{t}} \sin^2(\theta_n) \quad , \quad (G.3)$$

and

$$\tau_{RT} = \sigma_\infty \frac{A_F}{h\bar{t}} \sin(\theta_n) \cos(\theta_n) \quad . \quad (G.4)$$

As previously mentioned, the negative of these stresses will be applied to the boundary of the hole in order to remove the resultant stress on the hole boundary. Since it is only necessary to solve the axial equation in order to obtain the axial stresses and displacements, a boundary condition in the axial (fiber) direction is the only one needed. Thus the appropriate boundary condition can be derived by summing forces in the axial (y) direction.

$$\frac{A_F}{h\bar{t}} \sigma_F \Big|_n \sin(\theta_n) + \tau_{n+1} \cos(\theta_n) = -\sigma_\infty \frac{A_F}{h\bar{t}} \sin(\theta_n) \quad . \quad (G.5)$$

The same equation can be derived by summing forces in the radial and transverse directions and solving the resulting equation simultaneously.

The stresses can now be expressed in terms of displacements by using the shear-lag assumptions as before. Upon substitution, the new boundary condition becomes

$$\frac{A_F E_F}{G_M t} \frac{dV_n}{dy} \sin(\theta_n) + [V_{n+1} - V_n] \cos(\theta_n) = \frac{-\sigma_\infty A_F}{G_M t} \sin(\theta_n) . \quad (G.6)$$

From the geometry of the hole, as seen in figure (8), the radius can be expressed as

$$R = \frac{2N+1}{2} h, \quad (G.7)$$

where the coordinates of a particular point are

$$x_n = hn \quad \text{and} \\ y_n = h \sqrt{-n^2 + \left(\frac{2N+1}{2}\right)^2} . \quad (G.8)$$

The boundary condition for the circular hole then becomes

$$\frac{dV_n}{d\eta} + \frac{\alpha_n}{H_0 \sqrt{1-\alpha_n^2}} [V_{n+1} - V_n] = -1 , \quad (G.9)$$

where

$$\alpha_n = \frac{2n}{2N+1} \quad \text{and} \quad H_0 = \sqrt{\frac{A_F E_F}{G_M h t}} .$$

This boundary condition must be satisfied at the appropriate value along the boundary of the hole. It is seen that the normalized coordinate η is then

$$\eta(n) = \frac{Y_n}{hH_0} = \frac{2N+1}{2H_0} \sqrt{1-\alpha_n^2} . \quad (G.10)$$

Finally, the boundary condition becomes

$$\frac{2}{\pi} \int_0^{\pi} \sum_{m=0}^N B_m \cos(m\theta) \delta e^{-\delta \eta_n} \cos(n\theta) d\theta$$

$$+ \frac{\alpha_n}{H_0 \sqrt{1-\alpha_n^2}} \frac{2}{\pi} \int_0^{\pi} \sum_{m=0}^N B_m \cos(m\theta) e^{-\delta \eta_n} \{\cos[(n+1)\theta] - \cos(n\theta)\} = -1 .$$

(G.11)

This boundary condition replaces equation (B.46) used in the slit problem. Note that this solution is not independent of material properties due to the term H_0 defined above.

Since the damage is defined in the same manner as in section B for the slit, the integral equation for the present solution remains the same. The only other change is that the slit length (β) must be, at least, equal to the matrix mismatch on the last inclined element

This value is given by

$$\beta = \frac{1}{\left[2H_0 \sqrt{1-\alpha_n^2} \right]} .$$

(G.12)

The solution is obtained in the same manner as in the previous sections.

H. Two-Dimensional Shear-Lag Model with Broken Fibers for the Half-Plane

The motivation for much of the above work has been the interest in attempting to develop approximate analyses capable of predicting accurately the fracture behavior of hybrid (buffer strip) composite laminates. In this report solutions have been developed and the significance and validity of the various models will be demonstrated for the unidirectional full-plane laminate following this section. Based on the understanding developed in this phase of the study, future work will involve the extension of these models to multi-material laminates. As a first step in this direction the solution for adjoining unidirectional half-planes containing damage at, or near, the interface will be investigated. The solution presented below is a fundamental part of this extension, and consists of the solution for an edge crack in a unidirectional half-plane. Using superposition, i.e.; matching boundary conditions on the interface, this solution can then be added to a second half-plane having different fiber and matrix properties to construct the adjacent half-plane problem.

A two-dimensional array of parallel fibers with an arbitrary number of broken fibers at the free edge is shown in Figure (11). The laminate is subjected to a prescribed shear stress and transverse normal stress along the free edge in addition to a remote uniform tensile stress in the axial direction. No additional damage other than the broken fibers at the free edge is considered at this time.

With reference to the free-body diagrams shown in Figure (12) the equilibrium equations in the axial and transverse directions are given below. The boundary conditions on the free edge must now be specified

as opposed to the full-plane solution, in which they were accounted for by symmetry. We assume the first fiber in the half-plane to be embedded in the matrix material and, as seen in Figure (11), it will have a different set of equilibrium equations than all the remaining fibers.

The equations of equilibrium are:

$$\frac{A_F d\sigma_F|_1}{dy} + t \tau|_2 - t \tau_a = 0 , \quad (H.1)$$

and

$$\sigma_M|_2 - \sigma_M|_1 + \frac{h}{2} \frac{d}{dy} \left\{ \tau|_2 + \tau_a \right\} = 0 , \quad (H.2)$$

for the first fiber.

$$\frac{A_F d\sigma_F|_n}{dy} + t \tau|_{n+1} - t \tau|_n = 0 , \quad (H.3)$$

and

$$\sigma_M|_{n+1} - \sigma_M|_n + \frac{h}{2} \frac{d}{dy} \left\{ \tau|_{n+1} + \tau|_n \right\} = 0 , \quad (H.4)$$

for all other fibers.

Substituting the stress-displacement relations of Section A into the above equilibrium equations the following pairs of equations are obtained :

$$\frac{A_F E_F h}{G_M t} \frac{d^2 v_1}{dy^2} + (v_2 - v_1) - \tau_a \frac{h}{G_M} = 0 , \quad (H.5)$$

and

$$\frac{E_M}{h} (u_2 - u_1) - \sigma_M|_1 + \frac{G_M}{2} \frac{d}{dy} (v_2 - v_1) + \frac{h}{2} \frac{d}{dy} \tau_a = 0 , \quad (H.6)$$

for the first fiber.

$$\frac{A_F E_F h}{G_M t} \frac{d^2 v_n}{dy^2} + (v_{n+1} - 2v_n + v_{n-1}) = 0 , \quad (H.7)$$

and

$$\frac{E_M}{h} (u_{n+1} - 2u_n + u_{n-1}) + \frac{G_M}{2} \frac{d}{dy} (v_{n+1} - v_{n-1}) = 0 \quad (\text{H.8})$$

for all other fibers.

From equations (H.5) and (H.7) it can be observed that the axial equilibrium equations are independent of transverse displacement. Since only fiber axial displacements and axial stresses will be developed in this section, the solution for the transverse direction equilibrium equation will not be given here.

The same change of variables as in section A will be used to normalize the quantities in the equilibrium equations. The resulting equations in the nondimensional form are given by

$$\frac{d^2 V_1}{d\eta^2} + (V_2 - V_1) - \bar{\tau}_a = 0 ,$$

for the first fiber, and

$$\frac{d^2 V_n}{d\eta^2} + (V_{n+1} - 2V_n + V_{n-1}) = 0 , \quad (\text{H.9})$$

for all other fibers, where

$$\bar{\tau}_a = \sqrt{\frac{E_F t h}{A_F G_M}} \frac{\tau_a}{\sigma_\infty} .$$

Defining a new function $f_1(\eta)$ such that

$$f_1(\eta) = \bar{\tau}_a - V_1 , \quad (\text{H.10})$$

for all values of n the above two equations become

$$\frac{d^2 V_1}{d\eta^2} + V_2 - 2V_1 = f_1(\eta) , \quad (\text{H.11})$$

for the first fiber, and

$$\frac{d^2 V_n}{dn^2} + V_{n+1} - 2V_n + V_{n-1} = 0 \quad , \quad (H.12)$$

for all other fibers.

These differential-difference equations may be reduced to differential equations by introducing a new function $\bar{V}(n, \theta)$ such that the normalized displacement $V_n(n)$ is the Fourier coefficient in a Fourier series expansion. In order to represent the free-edge boundary conditions as discussed earlier, it is appropriate to utilize a sine transform. Then

$$\bar{V}(n, \theta) = \sum_{n=1}^{\infty} V_n(n) \sin(n\theta) \quad , \quad (H.13)$$

and

$$V_n(n) = \frac{2}{\pi} \int_0^{\pi} \bar{V}(n, \theta) \sin(n\theta) d\theta \quad . \quad (H.14)$$

With the introduction of $\bar{V}(n, \theta)$ the equilibrium equations become, respectively,

$$\frac{2}{\pi} \int_0^{\pi} \left\{ \frac{d^2 \bar{V}}{dn^2} - 2[1 - \cos(\theta)] \bar{V} \right\} \sin(\theta) d\theta = f_1(n) \quad , \quad (H.15)$$

and

$$\frac{2}{\pi} \int_0^{\pi} \left\{ \frac{d^2 \bar{V}}{dn^2} - 2[1 - \cos(\theta)] \bar{V} \right\} \sin(n\theta) d\theta = 0 \quad . \quad (H.16)$$

Making use of the orthogonality of circular functions these two equations may be written as one equation valid for all n as follows:

$$\begin{aligned} \frac{2}{\pi} \int_0^{\pi} \left\{ \frac{d^2 \bar{V}}{dn^2} - 2[1 - \cos(\theta)] \bar{V} \right\} \sin(n\theta) d\theta \\ = \frac{2}{\pi} \int_0^{\pi} f_1(n) \sin(\theta) \sin(n\theta) d\theta \quad . \end{aligned}$$

This equation is of the form

$$\frac{2}{\pi} \int_0^{\pi} F(\eta, \theta) \sin(n\theta) d\theta = 0 \quad , \quad \text{for all } \eta \text{ and } n \quad ,$$

and noting the definition of $\bar{V}(\eta, \theta)$ in equations (H.13) and (H.14) it is seen that the function $F(\eta, \theta)$ is odd valued in θ and, therefore, if the integral is to vanish for all n the function $F(\eta, \theta)$ must be zero.

The single equation specifying $\bar{V}(\eta, \theta)$ is then

$$\frac{d^2 \bar{V}}{d\eta^2} - \delta^2 \bar{V} = f_1(\eta) \sin(\theta) \quad , \quad (\text{H.17})$$

where

$$\delta^2 = 2[1 - \cos(\theta)] = 4 \sin^2(\theta/2) \quad .$$

As before, the solution to the problem of vanishing stresses and displacements at infinity and uniform compression on the ends of broken fibers will now be sought.

The boundary conditions are given by

$$V_n = 0 \quad \text{as} \quad \eta \rightarrow \infty \quad ,$$

for all fibers,

$$\frac{dV_n}{d\eta} = \bar{\sigma}_F \Big|_n = -1 \quad , \quad \text{at} \quad \eta = 0 \quad , \quad (\text{H.18})$$

for all broken fibers, and

$$V_n(0) = 0 \quad \text{at} \quad \eta = 0 \quad ,$$

for all unbroken fibers.

Equation (H.17) has the complete solution satisfying vanishing stresses and displacements remote from the damage as

$$\bar{V}(\eta, \theta) = A(\theta) e^{-\delta \eta} - \frac{\sin(\theta)}{\delta} \int_{\eta}^{\infty} \sinh[\delta(\eta-t)] f_1(t) dt \quad , \quad (\text{H.19})$$

where the functions $A(\theta)$ and $f_1(t)$ must be determined from the remaining boundary conditions. Using equation (H.14), the displacement is given by

$$V_n(\eta) = \frac{2}{\pi} \int_0^\pi \left[A(\theta) e^{-\delta\eta} - \frac{\sin(\theta)}{\delta} \int_n^\infty \sinh[\delta(\eta-t)] f_1(t) dt \right] \sin(n\theta) d\theta . \quad (\text{H.20})$$

The remaining boundary conditions give

$$\frac{dV_n(0)}{d\eta} = \frac{2}{\pi} \int_0^\pi \left\{ -\delta A(\theta) - \sin(\theta) \int_0^\infty \cosh[\delta(\eta-t)] f_1(t) dt \right\} \sin(n\theta) d\theta = -1 , \quad (\text{H.21})$$

for all broken fibers, and

$$V_n(0) = \frac{2}{\pi} \int_0^\pi \left\{ A(\theta) + \frac{\sin(\theta)}{\delta} \int_0^\infty \sinh(\delta t) f_1(t) dt \right\} \sin(n\theta) d\theta = 0 , \quad (\text{H.22})$$

for all unbroken fibers. Equation (H.22) is solved exactly by taking

$$A(\theta) + \frac{\sin(\theta)}{\delta} \int_0^\infty \sinh(\delta t) f_1(t) dt = \sum_{m=1}^N B_m \sin(m\theta) , \quad (\text{H.23})$$

where B_m are constants. Equation (H.22) then gives a system of N algebraic equations for N constants, B_m , in terms of $f_1(\eta)$ which is as yet unknown. Eliminating $A(\theta)$ between equations (H.20) and (H.23), the displacement $V_n(\eta)$ can be given as

$$V_n(\eta) = \frac{2}{\pi} \int_0^\pi e^{-\delta\eta} \sum_{m=1}^N B_m \sin(m\theta) \sin(n\theta) d\theta - \frac{1}{2} \int_0^\infty f_1(t) \left\{ C_n(|t-\eta|) - C_n(t+\eta) \right\} dt , \quad (\text{H.24})$$

where

$$C_n(\xi) = \frac{2}{\pi} \int_0^\pi \frac{\sin(\theta)}{\delta} e^{-\delta\xi} \sin(n\theta) d\theta$$

and

$$\delta = 2 \sin(\theta/2) .$$

Equation (H.21) then becomes

$$\frac{2}{\pi} \int_0^\pi \left\{ -\delta \sum_{m=1}^N B_m \sin(m\theta) + \sin(\theta) \int_0^\infty e^{-\delta t} V_1(t) dt - \sin(\theta) \int_0^\infty e^{-\delta t} \bar{\tau}_a(t) dt \right\} \sin(n\theta) d\theta = -1 , \quad (\text{H.25})$$

where $f_1(t)$ has been replaced by $\bar{\tau}_a - V_1(t)$.

Equations (H.10) along with (H.24) gives

$$V_1(\eta) = \frac{2}{\pi} \int_0^\pi e^{-\delta\eta} \sum B_m \sin(m\theta) \sin(\theta) d\theta + \frac{1}{2} \int_0^\infty \left\{ V_1(t) - \bar{\tau}_a(t) \right\} \left\{ C_1(|t-\eta|) - C_1(t+\eta) \right\} dt, \quad (H.26)$$

where

$$C_1(\xi) = \frac{2}{\pi} \int_0^\pi \frac{\sin^2(\theta)}{\delta} e^{-\delta\xi} d\theta.$$

Equations (H.25) and (H.26) must be solved simultaneously for $V_1(\eta)$ and the constants B_m . Once $V_1(\eta)$ and B_m are known, the displacement of any fiber n can be obtained from equation (H.20) and hence the fiber stresses.

These equations were solved as follows:

- (I) An initial set of constants B_m was determined by setting $f_1(t) = 0$, that is, $V_1(t) = \bar{\tau}_a(t)$ in equation (H.25) giving

$$\frac{2}{\pi} \int_0^\pi \left\{ -\delta \sum_{m=1}^N B_m \sin(m\theta) \sin(n\theta) \right\} d\theta = -1, \quad n = 1, 2, \dots, N. \quad (H.27)$$

- (II) These initial constants were then substituted into the integral equation (H.26) and the function $V_1(t)$ was determined for a known distribution of $\bar{\tau}_a(t)$.
- (III) Using $V_1(t)$, a new set of constants B_m was computed from equation (H.25).

- (IV) This procedure was repeated until the unknowns changed less than a prescribed amount with the additional iterations.

In the above solution, the unknown function, $V_1(\eta)$ was assumed to be piecewise parabolic over the interval $0 \leq \eta \leq \infty$ of the form

$$V_1^i(\eta) = \gamma_0^i + \gamma_1^i \eta + \gamma_2^i \eta^2, \quad i = 1, 2, \dots, k$$

when the interval was divided into k subdivisions. The function, $V_1(\eta)$ contained $3k$ unknowns. $(k+1)$ equations are obtained by requiring that the integral equation (H.26) be satisfied at the $(k+1)$ end points, $(2k-2)$ equations resulted from the requirement of continuity of the function $V_1(\eta)$ and its first derivative between adjacent intervals and the last equation was given by setting $V_1(\eta) = 0$ as $\eta \rightarrow \infty$. Because the interval of integration was infinite, the piecewise linear approximation for $V_1(\eta)$ unlike in the preceding sections was found to be inadequate.

SOLUTIONS AND RESULTS

Numerical solutions have been developed for all the specific problems discussed in the previous sections, using an IBM 370 computer at Clemson University. For the case of a notch with no additional transverse or longitudinal damage, as considered in section A, the solution involves inverting the system of algebraic equations (A.21) for the constants, B_m . In sections B-G the inclusion of longitudinal damage requires the introduction of an unknown function $g(\eta)$ representing the displacement difference between adjacent fibers in the damage zone. Satisfaction of the boundary conditions then gives a far more complex system of algebraic equations for the constants B_m , coupled with a Fredholm integral equation for the function $g(\eta)$. The form of this pair of equations is identical for all sections B-G (see equations (B.46), (B.47), and (B.48)). The solution technique discussed in section B for these equations is appropriate for the remaining sections through G. For the half-plane considered in section H, even though no longitudinal damage is assumed, a set of equations similar to those of sections B-G still results. A discussion of an appropriate solution technique for the half-plane is given at the end of section H and some changes made necessary by unbounded intervals of integration are considered.

For the present report the main emphasis will be to compare the results of the various models and demonstrate the agreement with available experimental results. More detailed results for the original Hedgepeth problem are given in [1]; the inclusion of longitudinal damage for one broken fiber is given in [2] and [3], and the general solution of section B is presented in [9].

Some interesting observations concerning the case of broken fibers with no additional damage, as presented in section A and [1] are first considered, with particular emphasis on the behavior of the fiber stress in front of the notch. The normalized fiber stress in the first unbroken fiber was shown in [1] to have the following representation:

$$K_r = \frac{\sigma_F}{\sigma_\infty} = \frac{4.6.8.....(2r + 2)}{3.5.7.....(2r + 1)} \quad (1)$$

where σ_F is the stress in the first unbroken fiber, and r is the total number of broken fibers. This equation may be written as

$$K_r = \frac{(2)^{2r} (r + 1)! (r)!}{(2r + 1)!} \quad (2)$$

Using Stirling's formula for the asymptotic representation of $(r)!$ when r is large, i.e.

$$(r)! \rightarrow \sqrt{2\pi r} \left(\frac{r}{e}\right)^r,$$

and substituting into equation (2), gives

$$K_r = \frac{\sqrt{\pi}}{2} \sqrt{r} \quad (3)$$

If the total number of broken fibers is odd and the notch is symmetric about the y -axis, as is the case in all the full-plane problems considered here, then $r = 2N + 1$, where N is the last broken fiber, so that equation (3) may be written as

$$\bar{\sigma}_F|_{N+1} = \frac{\sqrt{\pi}}{2} \sqrt{2N + 1} = \sqrt{\frac{\pi}{2}} \sqrt{N}, \text{ for large } N. \quad (4)$$

The present failure criterion is similar to the "point stress" criterion presented by Nuismer and Whitney in [15], at least when applied to the models of sections A and B. That is, if transverse damage is not admitted then laminate failure is assumed to occur when the stress in the first unbroken fiber reaches the unnotched ultimate stress. The

remote failure stress, σ_∞ , is then given by equation (1) for any number of broken fibers, r , where σ_F is replaced by the unnotched strength σ_0 . Following [15], a fracture toughness parameter can be defined as $K_Q = \sigma_\infty \sqrt{\pi a}$ where a is the crack half-length. K_Q is given by equation (4) for large crack lengths as

$$K_Q = \sigma_\infty \sqrt{\pi a} = \sigma_0 \sqrt{2d}, \quad (5)$$

where d is the fiber spacing, $a \approx Nd$, and $\sigma_\infty = \sigma_0 \sqrt{2/\pi N}$.

A comparison can also be made between the solution of section A and that of a homogeneous isotropic plate with a central notch of length $2a$ (Griffith crack). The stress distribution at the crack tip along the x -axis is given by

$$\frac{\sigma_y}{\sigma_\infty} = \frac{x}{\sqrt{x^2 - a^2}}, \quad x \geq a \quad (6)$$

This equation can be modified for a unidirectional lamina in terms of the discrete fiber spacing and fiber index as

$$\bar{\sigma}_F \Big|_n = \frac{nd}{\sqrt{(nd)^2 - (N + C_N)^2 d^2}} = \frac{n}{\sqrt{n^2 - (N + C_N)^2}}, \quad n \geq N + 1, \quad (7)$$

where

$\bar{\sigma}_F \Big|_n$ is the normalized stress in the fiber n ,

d is the fiber spacing,

n is the fiber index

N is the index of the last broken fiber, and,

C_N is a constant needed to fit the data for each particular initial notch length specified by N . Note that $(N + C_N)d$ represents an equivalent notch half-length.

For $n = N + 1$ this equation is set equal to equation (2), with $r = 2N + 1$, in order to determine the constant C_N for any particular N . The following table of values for C_N as a function of N results:

| N | 0 | 1 | 10 | 1000 | |
|-------|--------|--------|--------|--------|-----------------------|
| C_N | 0.6614 | 0.6742 | 0.6805 | 0.6814 | 0.6815 |
| | | | | | $(1 - \frac{1}{\pi})$ |

For large N equation (7), with $n = N + 1$, and equation (4) in place of equation (2) gives the limiting values of C_N as

$$\lim_{N \rightarrow \infty} \frac{N + 1}{\sqrt{(N + 1)^2 - (N + C_N)^2}} = \frac{\pi}{2} \sqrt{N},$$

from which

$$C_N = 1 - \frac{1}{\pi} = 0.6815 = C. \quad (8)$$

It is then seen that C_N is approximately equal to a constant, C , independent of N . Now, using the above values for C_N the stress in fibers $n > N + 1$ in front of the notch was computed from equation (7) and compared with the solution of section A. For all notch lengths the agreement was found to be excellent as shown in Figure (13). Therefore the central notch in a unidirectional laminate using the shear-lag model has a square-root type stress distribution with an equivalent notch length given by $(N + C_N)d$ where the constant $C_N \approx C = 1 - 1/\pi$ for all N . That is, the stress in the first unbroken fiber is given by the modified Griffith solution, equation (7), which also correctly predicts the stresses in the remaining unbroken fibers.

An analogous investigation concerning the maximum fiber stress and the fiber stress decay away from the notch when longitudinal and transverse damage is present, as given in sections B and C, is now discussed. The results are considerably different from the above and it is indicated that a basic assumption of [15] in which a square-root behavior was assumed to exist may be in error. That is, for cases having longitudinal and/or transverse damage the notch tip fiber stress as determined from sections B and C does not have a square-root form. To demonstrate this for longitudinal damage we used equation (7), with $n = N + 1$, to represent the fiber stress in front of the notch and determined the constant C_N by comparing with the numerical results. A significantly different value of C_N was found for each particular N as indicated in the following table. In constructing this table the ultimate stress in fiber $N + 1$ was taken as constant for all values of N ; the remote stress and damage length, α , then changed with N .

| N | 0 | 1 | 3 | 14 |
|-------|--------|--------|--------|---------|
| C_N | 0.6459 | 0.5008 | 0.3437 | -0.2364 |

Further, using a specific value of N and the corresponding C_N , the fiber stress computed for $n > N + 1$ from equation (7) was found to be different from the numerical results. An example of the fiber stress for seven broken fibers, and longitudinal damage consisting of yielding given by $\alpha = 5.0$ is given in Figure (13). First, comparing with the results of the no damage, it is seen that the stress distribution is greatly reduced and distributed more uniformly to the adjacent fibers.

Second, the results are seen to be different from equation (7) but not drastically so.

When transverse damage is included the stress field, shown in Figure (13) for four damaged fibers, is fundamentally different from that of the modified Griffith form, equation (7). A value of C_N was not determined. It is indicated below that both longitudinal yielding and transverse damage are necessary in order to agree with the limited experimental results for boron/aluminum laminates.

The failure criterion for longitudinal damage alone is the same as in section A. When the stress in the first unbroken fiber reaches the unnotched laminate stress and fails, then the stress in the adjacent unbroken fiber will be above the critical value.

If transverse damage is also present the failure criterion is more complicated. The results from the model developed in section C indicated that stable transverse fiber breaks can occur. Failure of the first fiber does not then necessarily signify lamina failure as it may well require an increased applied stress to critically stress the next fiber. Recall that in the lamina, the fiber breaks occur in front of but not necessarily in line with the initial notch, with the matrix material remaining intact. Shear stress transfer from the matrix as well as some small axial matrix stress then gives a reduced load carrying capacity to the damage region in front of the notch as accounted for by the stiffness coefficient, γ . Typical results are shown in Figure (14) for an initial notch length corresponding to seven broken fibers and a fiber stress in the damaged zone corresponding to a stiffness coefficient of $\gamma = 0.90$. It is seen that the transverse damage is

stable until about seven additional fibers are broken. At this point the curve levels off and successive breaks require no increase in applied stress, σ_{∞} . An appropriate failure criterion is then to determine the applied stress, σ_{∞} , giving unstable transverse damage. It is significant that the number of stable fiber breaks was approximately constant, independent of initial notch length. This constant damage zone size was about seven broken fibers which is in good agreement with the observed results of Awerbuch and Hahn [13].

The value of γ , which represents the stress carried by the transverse damage region, was found to be that giving the best fit to the COD and strength curves along with a constant damage zone length. As the initial notch length increased, the load carried by the transverse damage region decreased, while the size of the region remained constant. Extensive experimental studies to investigate this behavior are underway.

The results of the present methods are shown below to predict accurately the fracture behavior of both brittle and ductile matrix composites in terms of crack opening displacement (COD) and fracture strength. It then seems reasonable to conclude that the manner of stress distribution in the fibers is given with the same degree of accuracy. If this is true then it follows that, for the notched laminate with longitudinal and transverse damage, the fiber stresses in front of the notch are less severe than a square-root behavior. The failure criteria suggested by Nuismer and Whitney [15], either the "point stress" or the "average stress" criterion both assume a stress field in the front of the notch as

$$\frac{\sigma_F}{\sigma_\infty} = \frac{x}{\sqrt{x^2 - a^2}} ; \text{ (see equation (10) of [15])},$$

where a is the half notch length. Based on the above observations these criteria are perhaps not valid for unidirectional laminates. It appears then that longitudinal and/or transverse damage reduces the influence of a notch to a greater degree than an equivalent notch length model, with a square-root behavior, would predict. It is important to note that, even though the present study indicates the true fiber stress distribution, section C, to be different from [15], results using the classical square-root behavior do predict the fracture characteristics of laminates with surprising accuracy. For example, see the work of Poe and Sova presented in references [16] and [17]. This is perhaps fortuitous as the stress is not drastically different from a square-root form even though only the undamaged laminate of section A agrees accurately with the square-root behavior of equation (7).

It has been demonstrated in [9] that for composites with a brittle matrix such as epoxy, the extensive splitting and the eventual instability in the longitudinal direction can be predicted by introducing longitudinal damage alone as covered in section B. Results for cases of one and seven broken fibers are presented in Figure (15).

For a composite with a ductile matrix such as aluminum some negligible splitting has been observed [14] and [1], but the stress in the fibers continues to increase with increased remote stress until the ultimate fiber stress is reached. In order to predict the fracture behavior of composites with a ductile matrix, such as boron/aluminum, it was found to be necessary to improve the model presented in section B.

Effectiveness of these improved models, which are developed in sections C-E, will now be discussed.

In all these cases, the model parameters such as number of constrained fibers, stiffness coefficient, strain-hardening ratio, and constraint ratio were varied and their effect on the fracture characteristics of the laminate was investigated. A comparison of predicted values with the experimental results of [13] was done with respect to two fundamental characteristics, crack opening displacement and laminate strength.

As explained in section B, the fiber axial displacement and stresses can be computed for different material properties, applied stress, and notch lengths. For a particular laminate a plot of COD vs applied load was obtained and then, by comparing with the experimental study of Averbuch and Hahn in [13] for the unidirectional boron/aluminum laminate, appropriate values of τ_0 and the stiffness constant G_M/h were determined. The laminate used in [13] had the following material and geometric properties:

$$E_F = 475 \times 10^9 \text{ Pa,}$$

$$A_F = 1.59 \times 10^{-8} \text{ m}^2 \quad (D = 0.1427 \text{ mm}),$$

$$t = 0.165 \text{ mm/ply, eight plies}$$

$$\sigma_{ult} = 3.98 \times 10^9 \text{ Pa}$$

$$w = \text{width} = 25.4 \text{ mm and}$$

$$\text{fiber center line spacing} = 0.178 \text{ mm.}$$

For a laminate having seven broken fibers, which corresponds to a notch length of about 1.27 mm, the load vs COD curve required specific values of τ_0 and G_M/h in order to give a "best fit" to the experimental

results of [13]. The numerical values of G_M/h and τ_o determined in this manner are given in the following table for the various models:

| | longitudinal damage, B | transverse damage, C | constraint layer, D | strain hardening, E |
|----------|-------------------------------------|------------------------------------|------------------------------------|-------------------------------------|
| G_M/h | $65.4 \times 10^{12} \text{ N/m}^2$ | $115 \times 10^{12} \text{ N/m}^2$ | $148 \times 10^{12} \text{ N/m}^2$ | $35.9 \times 10^{12} \text{ N/m}^2$ |
| τ_o | $109 \times 10^6 \text{ N/m}^2$ | $88 \times 10^6 \text{ N/m}^2$ | $82 \times 10^6 \text{ N/m}^2$ | $164 \times 10^6 \text{ N/m}^2$ |

For the strain-hardening case the modulus ratio was taken as $G_R = 0.5$ and for the constraint layer $C_R = 0.05$. Using the above tabulated values in each model gave essentially the same COD curves for both seven and twenty-nine broken fibers with both being in close agreement with the experimental results of [13]. This comparison is shown in Figure (16).

The differences in the four models in predicting COD curves is then small although the particular values of the material constants G_M/h and τ_o are considerably different as seen from the table.

Now using the above constants for G_M/h and τ_o , the normalized ultimate fiber stress

$$S = \frac{\sigma_{ult}}{\tau_o} \sqrt{\frac{G_M A_F}{E_F h t}}$$

was computed for a specific ultimate fiber stress. Then the remote stress required to give a particular ultimate stress in the first unbroken fiber, or unstable extension in the case of section C, was determined from a plot of applied stress, σ_∞ , vs fiber stress, σ_F , Figures (17) and (18). This gives the strength of the laminate as a function of number of broken fibers (or notch length). This was repeated for all

the models in sections B through E. Figure (19) shows the plot of applied stress as a function of number of broken fibers for the different models along with the experimental results of [13].

From Figure (19) it may be observed that even though COD was insensitive to model parameters, the strength curve was very much dependent on them. All the models predict the same trend in strength curves as those given by the experimental results. However, for the case of longitudinal damage, the model gives a much larger decrease in strength for small notch lengths than the experiment. At longer notches the model predicts the failure stress reasonably well. An increase in the fiber ultimate stress tends to rotate the curve about the knee of the curve without much change in the behavior for the shorter notches.

Addition of a constraint layer does not make a significant difference in the predicted strength curve. Variation in the constraint ratio had a similar effect as that of increasing the fiber ultimate stress in the longitudinal damage model.

The strain-hardening model predicts strength values much lower than those of the longitudinal damage model, making it more and more notch sensitive. The best predicted values of the strain-hardening model are no better than those of the longitudinal damage model.

The transverse damage model, however, predicts strength values very close to the experimental results and seems to account for an essential damage mode. By varying the transverse stiffness coefficient and number of constrained fibers, it was possible to move the predicted strength curve such that it fit the experimental results exceptionally well. One important observation was that the number of constrained fibers required

to fit the experimental data was approximately a constant at all notch lengths, indicating that the transverse damage zone size ahead of the notch tip was independent of the notch size.

Introduction of transverse damage in addition to longitudinal damage then not only predicts COD in good agreement, at the same time it predicts strength values exceptionally well. The above computed value of τ_0 is close to the yield stress for a homogeneous aluminum specimen. The equivalent stiffness, G_M/h , for $h = 1.78 \times 10^{-4}$ m (i.e., the center-line distance between fibers) gives a shear modulus of $G_M = 20.5 \times 10^9$ N/m² which is also close to the shear modulus of aluminum. For annealed aluminum the yield stress is about 95×10^6 N/m² and the shear modulus is 27×10^9 N/m².

Also of interest is the extent of the longitudinal yielding which is given by

$$\tilde{L} = \frac{L}{d} = \sqrt{\frac{E_F A_F h}{G_M t}} \frac{\alpha}{d} = 3.54 \text{ fiber spacings.}$$

For the case of seven broken fibers the damage length corresponds to $\alpha = 11.5$ or, therefore, $\tilde{L} = 40.7$ fiber spacings (approximately 6 times the crack length). For twenty-nine broken fibers $\alpha = 35$, and $\tilde{L} = 123.9$ fiber spacings (approximately 4 times the crack length). Experimental determination of the extent of longitudinal yielding is now being investigated by the writers; however, this damage does seem reasonable.

With the above observations in mind it should be emphasized that in order to predict the fracture behavior of unidirectional composites with a ductile matrix it was essential to consider the transverse damage of

matrix and fibers along with the longitudinal matrix damage as modeled in section C of this report.

Note that the above results indicate an approximately constant transverse damage zone size of seven fibers, independent of initial notch length, which is in agreement with both Awerbuch and Hahn [13] and Nuismer and Whitney [15]. However, the disagreement with Nuismer and Whitney [15] as discussed above is that the present solutions predict fiber stresses in front of the notch to be different from and less severe than a square-root behavior.

The final results to be presented in this report concern the solutions developed in sections F and G for the rectangular and circular cut-outs. Of principal interest will be the comparison of these results with the corresponding solutions for the notch. Extensive results are presented by Jones [18] where it is demonstrated that very little difference exists between the three solutions concerning maximum fiber stress and the stress distribution in front of the damage.

In Figure (20) results are presented for eleven broken fibers in the instance of no additional damage. The differences are largest in this case; any longitudinal or transverse damage brings the solutions closer together. Figure (21) gives the results for the same geometry with longitudinal damage, $\alpha = 4$, and transverse damage of four fibers. In both cases the material constant, H_0 , needed in the solution for the circular hole, was taken as 5.0 which corresponds to a volumetric ratio of 50% and $E_F/G_M = 50$. Within the range of realistic material properties for fiber dominated laminates, changes in H_0 have little effect on the solution.

The behavior depicted by these two figures is typical of the general results and one can conclude that the shape of the initial damage is less significant in determining the laminate fracture properties than the total number of fibers broken. These results are fundamentally different from the case of an isotropic plate in which the sharp notch has singular stresses near the notch tip with a square-root singularity; the rectangular hole also has singular stresses but with a power of less than one-half; and the circular hole has a stress concentration of three, independent of hole size.

Future work in the area of this study will include a detailed experimental investigation of the damage growth in notched boron/aluminum unidirectional laminates and the extension of the above half-plane solution to include damage and the presence of an adjacent half-plane of different material properties.

REFERENCES

- [1] Hedgepeth, J. M.: Stress Concentrations for Filamentary Structures. NASA TN D-882, 1961.
- [2] Hedgepeth, J. M.; and Van Dyke, P.: Local Stress Concentrations in Imperfect Filamentary Composite Materials. J. Comp. Mater., Vol. 1, 1967, pp. 294-309.
- [3] Van Dyke, P.; and Hedgepeth, J. M.: Stress Concentrations from Single Filament Failures in Composite Materials. Textile Research, Vol. 39, 1969, pp. 613-626.
- [4] Zweben, C.: Fracture Mechanics and Composite Materials: A Critical Analysis. Special Tech. Publ. 521, A.S.T.M., 1973, pp. 63-97.
- [5] Zweben, C.: An Approximate Method of Analysis for Notched Uni-directional Composites. Engineering Fracture Mechanics, Vol. 6, 1974, pp. 1-10.
- [6] Eringen, A. C.; and Kim, B. S.: Stress Concentration in Filamentary Composites With Broken Fibers. Princeton University Tech. Rep. No. 36, Sept. 1973, ONR Contract N-00014-67-A-0151-0004.
- [7] Franklin, H. G.: Hole Stress Concentration in Filamentary Structures. Fiber Science and Technology, Vol. 2, 1970, pp. 241-249.
- [8] Kulkarni, S. V.; Rosen, B. W.; and Zweben, C.: Load Concentration Factors for Circular Holes in Composite Laminates. J. Comp. Mater., Vol. 7, 1973, pp. 387-393.
- [9] Goree, J. G.; and Gross, R. S.: Analysis of a Unidirectional Composite Containing Broken Fibers and Matrix Damage. Engineering Fracture Mechanics, Vol. 13, 1979, pp. 563-578.
- [10] Goree, J. G.; and Gross, R. S.: Stresses in a Three-Dimensional Uni-directional Composite Containing Broken Fibers. Engineering Fracture Mechanics, Vol. 13, 1980, pp. 395-405.
- [11] Goree, J. G.; and Wilson, E. B., Jr.: Transverse Shear Loading In An Elastic Matrix Containing Two Elastic Circular Cylindrical Inclusions. J. Appl. Mech., Vol. 34, 1967, pp. 511-513.
- [12] Goree, J. G.; and Gross, R. S.: Stresses in a Three-Dimensional Uni-directional Composite Containing Broken Fibers. NASA CR-158986, NSG-1297, 1978.
- [13] Awerbuch, J.; and Hahn, H. T.: Fracture Behavior of Metal Matrix Composites. Proc. of the Soc. of Engr. Sci., Recent Advances in Engr. Sci., 1977, pp. 343-350.

- [14] Peters, P.: Fracture Mechanical Investigations on Uni-directional Boron-Aluminum and Boron-Epoxy Composites. J. Comp. Mater., Vol. 12, 1978, pp. 250-261.
- [15] Nuismer, R. J.; and Whitney, J. M.: Uniaxial Failure of Composite Laminates Containing Stress Concentrations. Fracture Mechanics of Composites, ASTM STP 593, American Society for Testing and Materials, 1975, pp. 117-142.
- [16] Sova, J. A.; and Poe, C. C., Jr.: Tensile Stress-Strain Behavior of Boron/Aluminum Laminates. NASA TP-1117, 1978.
- [17] Poe, C. C., Jr.: A Single Fracture Toughness Parameter for Fibrous Composite Laminates. NASA TM-81911, 1981.
- [18] Jones, W. F.: Uni-directional Composite Laminate with Circular and Rectangular Cut-outs. M.S. Thesis, 1981, Engineering Mechanics, Clemson University.

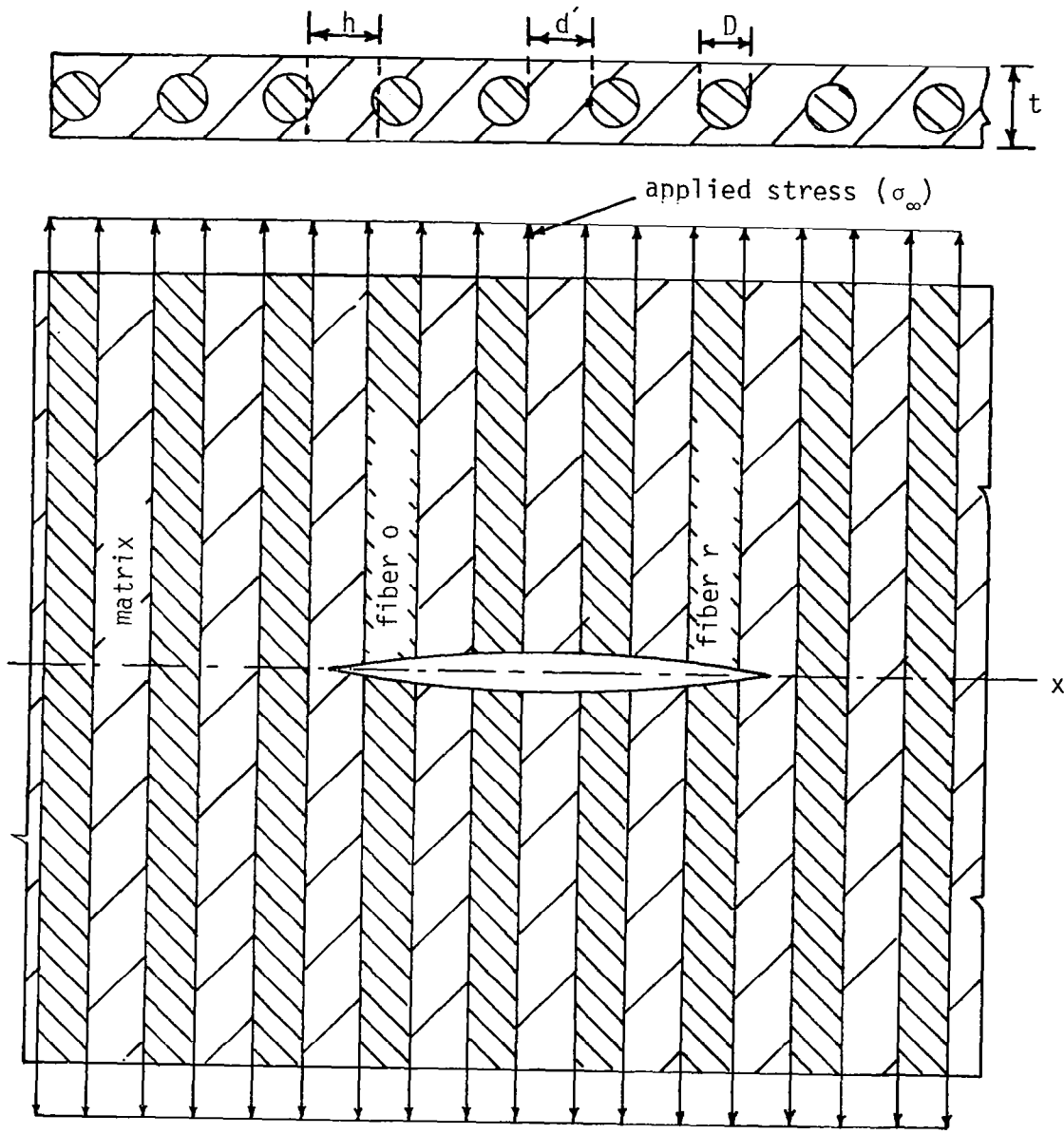


Figure 1. Two-dimensional unidirectional lamina with broken fibers.

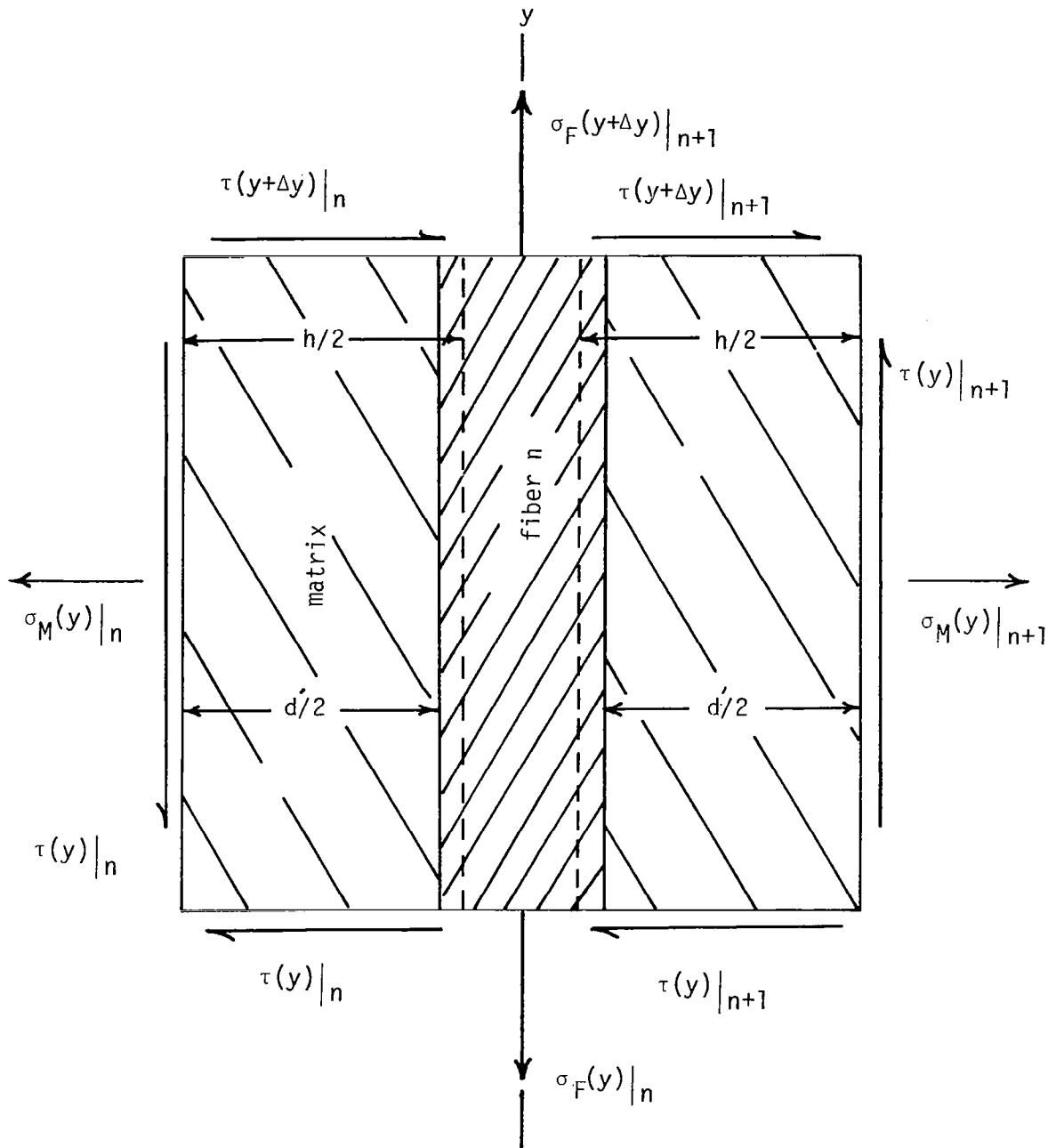


Figure 2. Free-body diagram of a typical element.

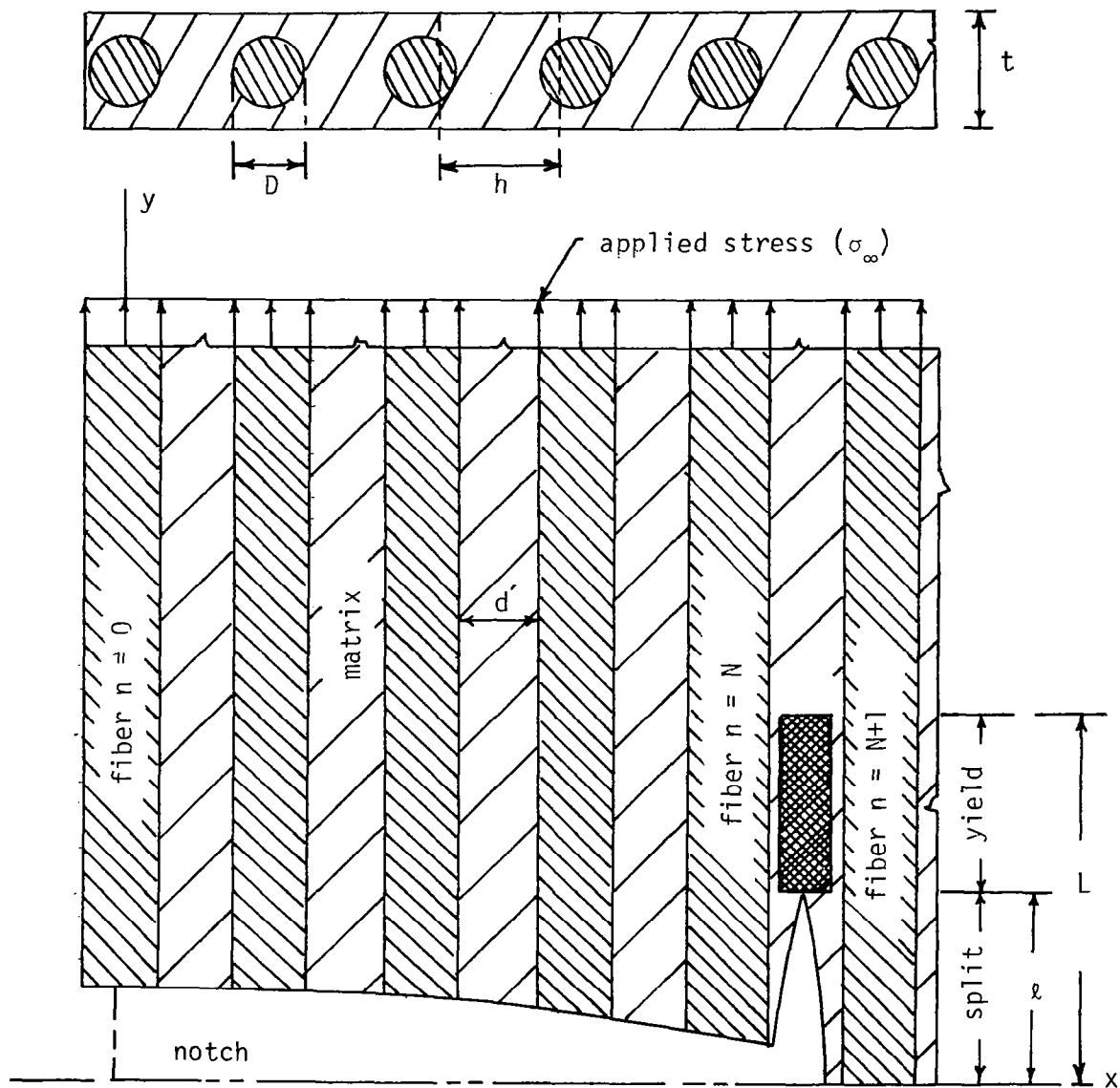


Figure 3. Two-dimensional unidirectional lamina with broken fibers and longitudinal matrix splitting and yielding (first quadrant).

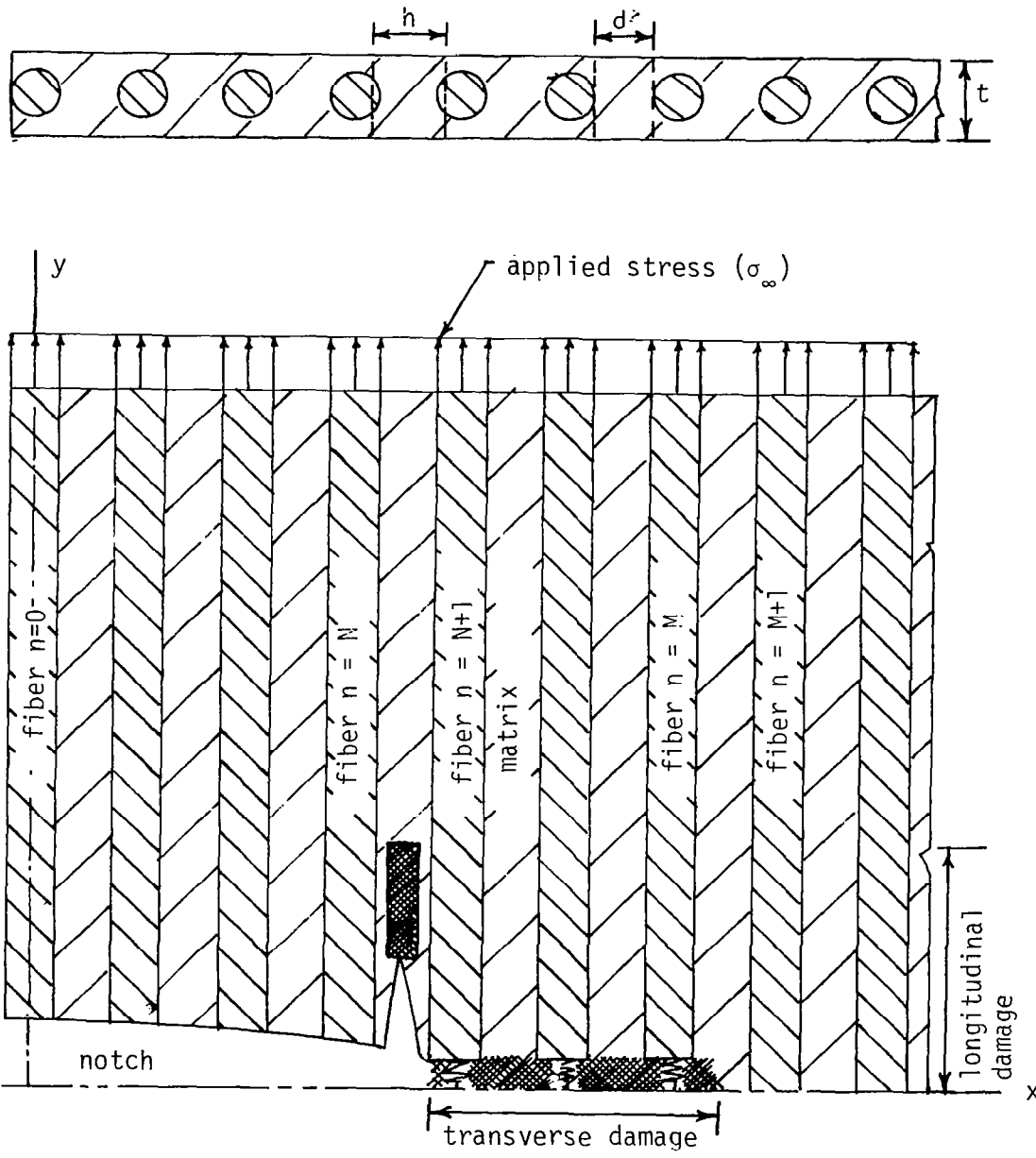


Figure 4. Two-dimensional unidirectional lamina with broken fibers, longitudinal matrix splitting and yielding and transverse fiber and matrix damage (first quadrant).

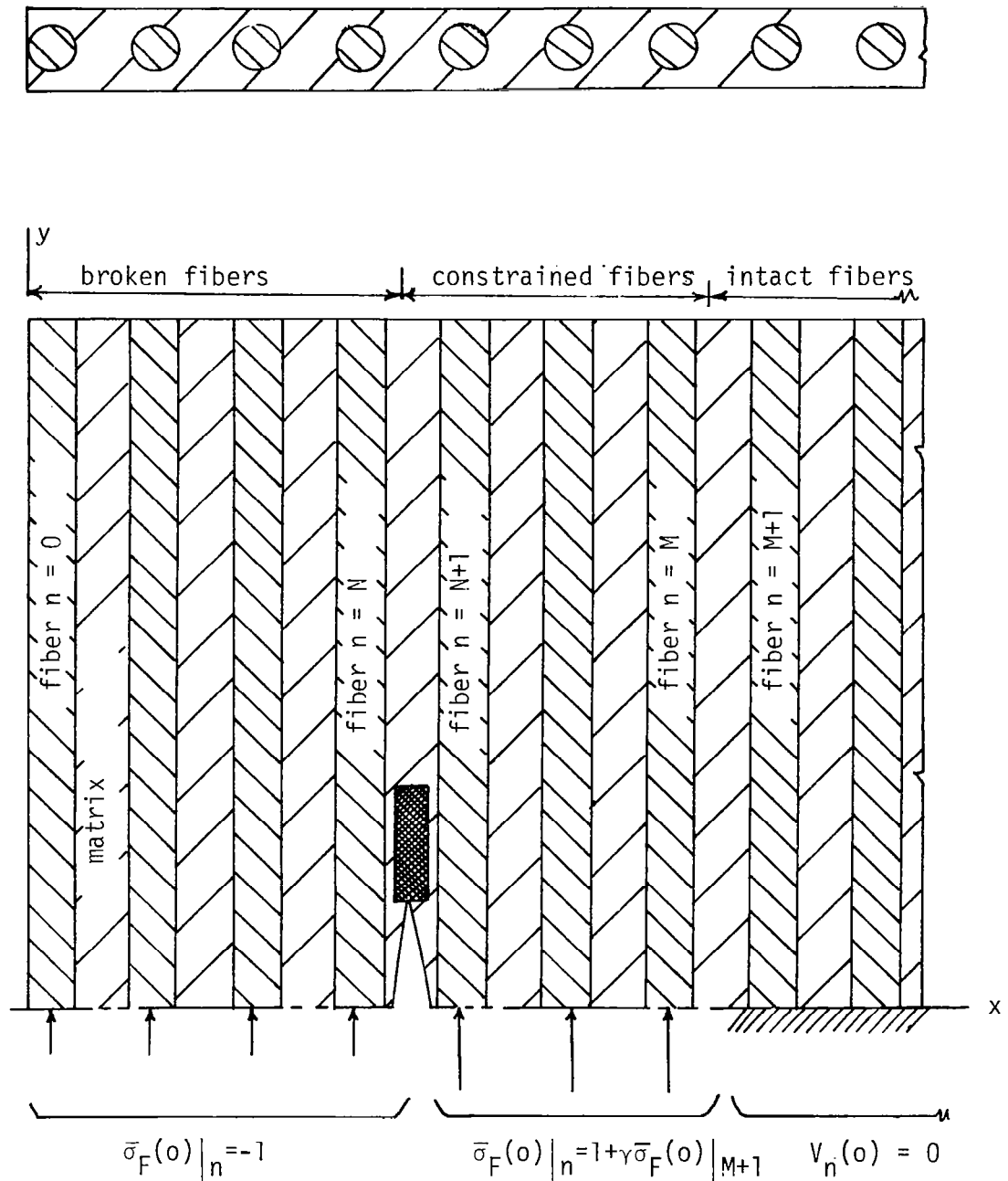
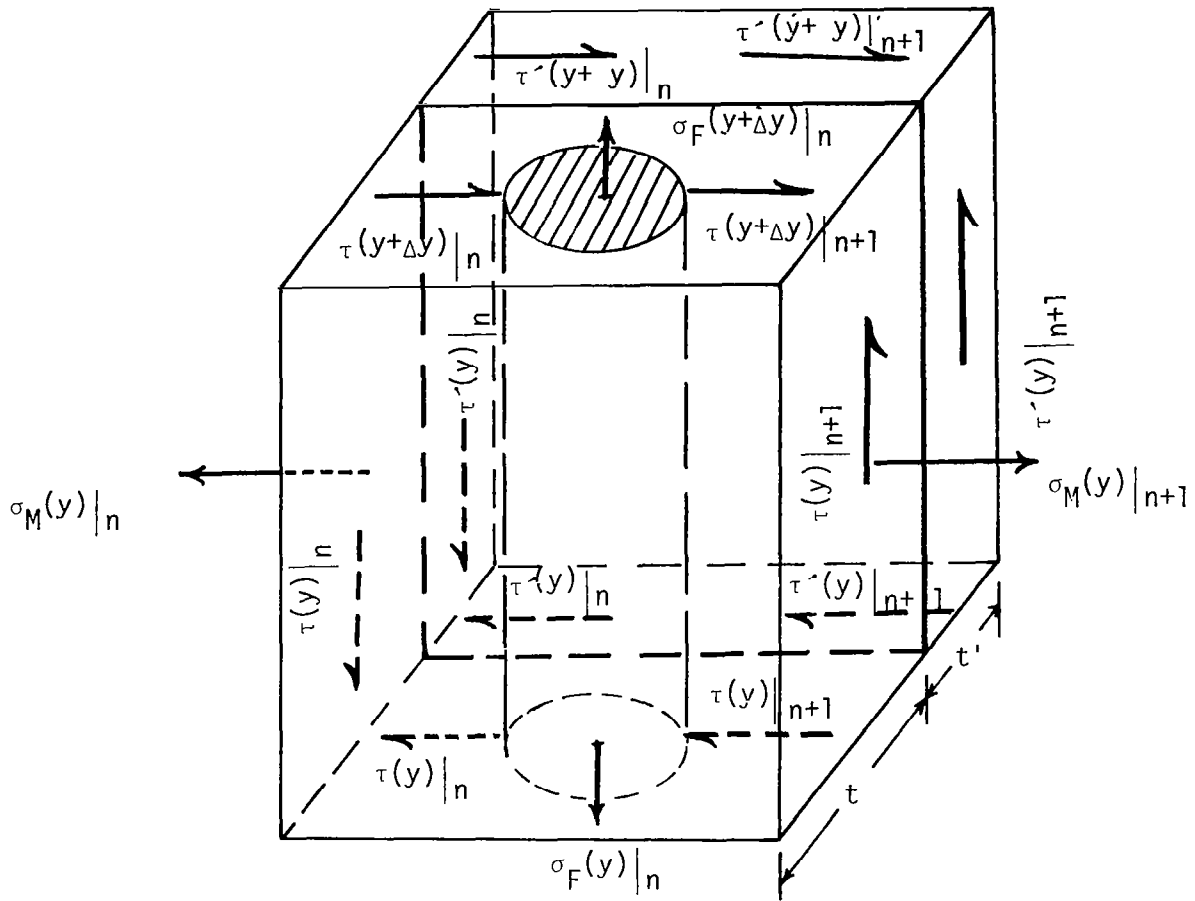


Figure 5. Boundary conditions along the x-axis for the transverse damage model.



- t = thickness of the main lamina
- t' = thickness of the constraint layer
- G_M/h = effective shear stiffness of the main lamina
- G'/h' = effective shear stiffness of the constraint layer
- $C_R = \frac{(G'/h')t'}{(G_M/h)t} = \text{Constraint ratio}$

Figure 6. Free-body diagram of an element consisting of the main lamina and the constraint layer.

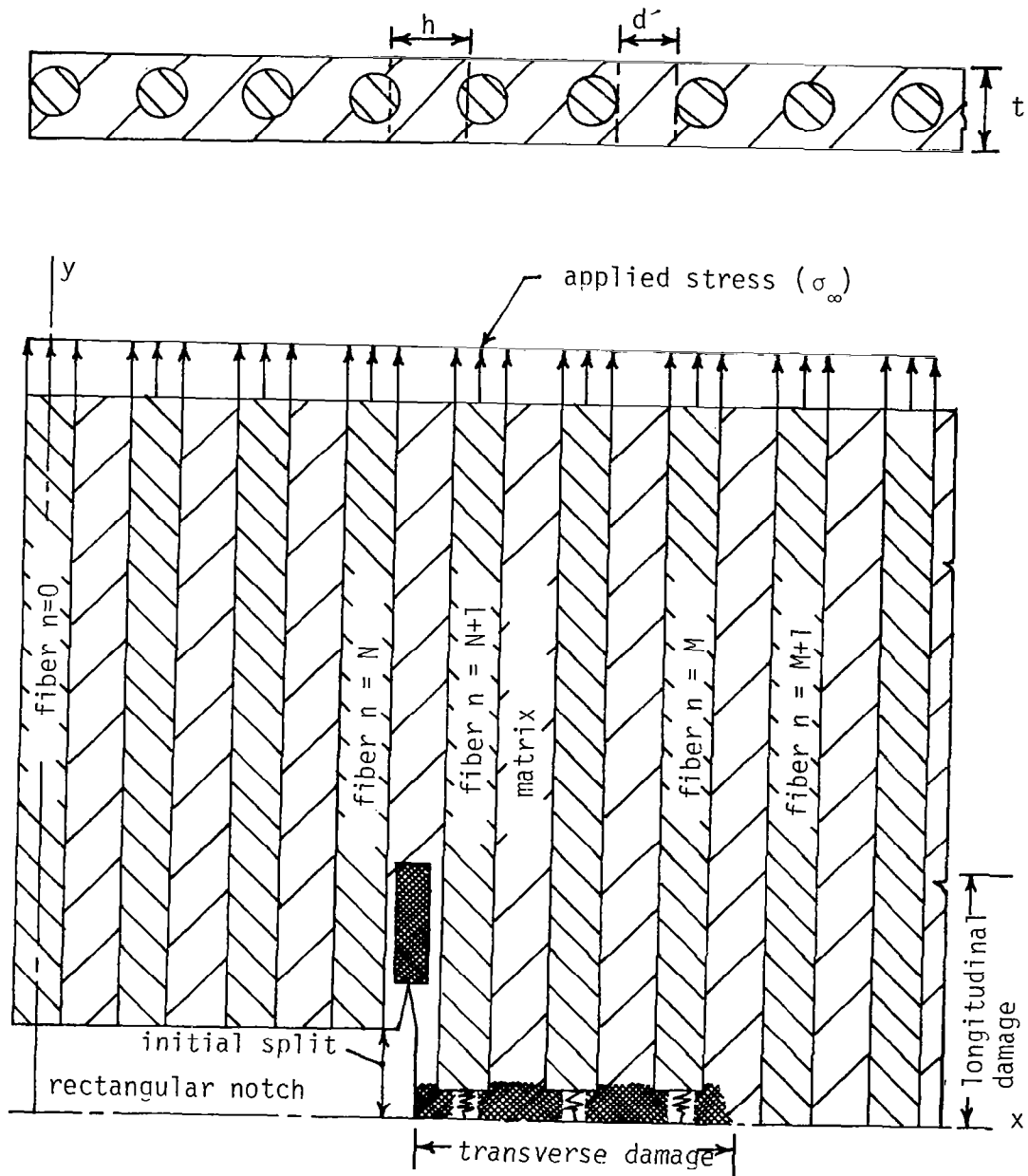


Figure 7. Two-dimensional unidirectional lamina with a rectangular notch, longitudinal matrix splitting and yielding and transverse damage (first quadrant).

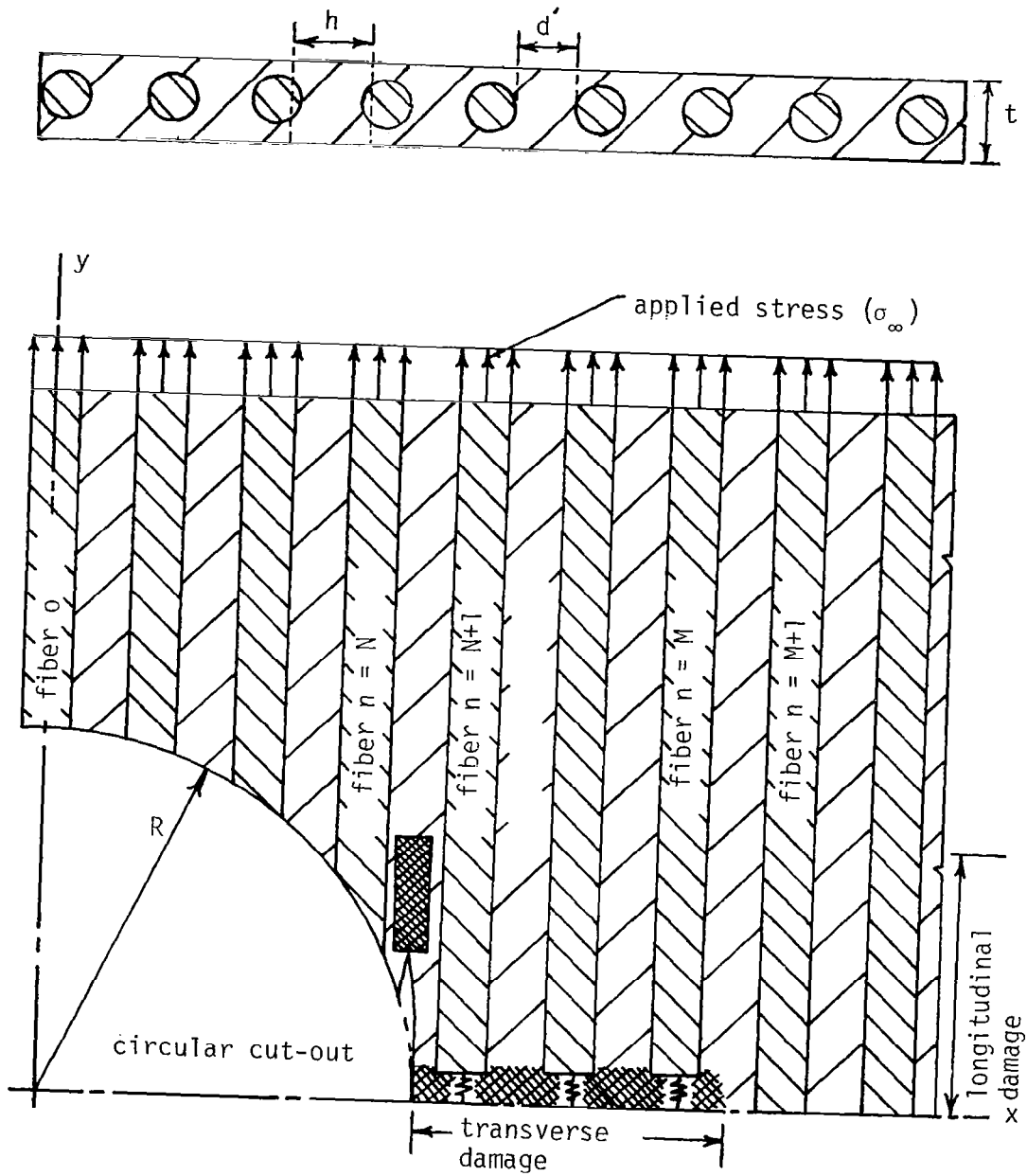


Figure 8. Two-dimensional unidirectional lamina with a circular cut-out, longitudinal matrix splitting and yielding and transverse damage (first quadrant).

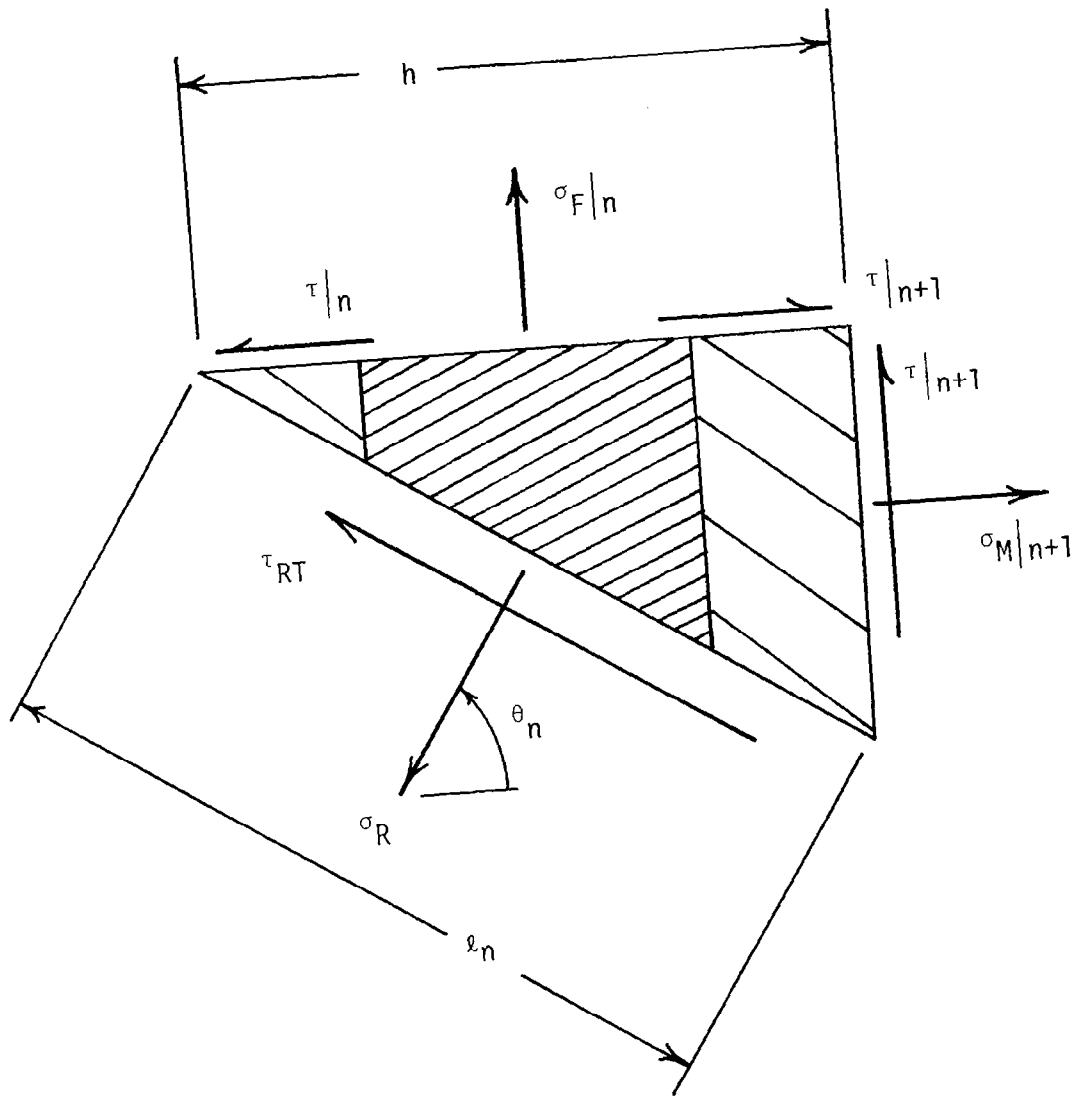


Figure 9. Free-body diagram of a typical element at the circular cut-out.

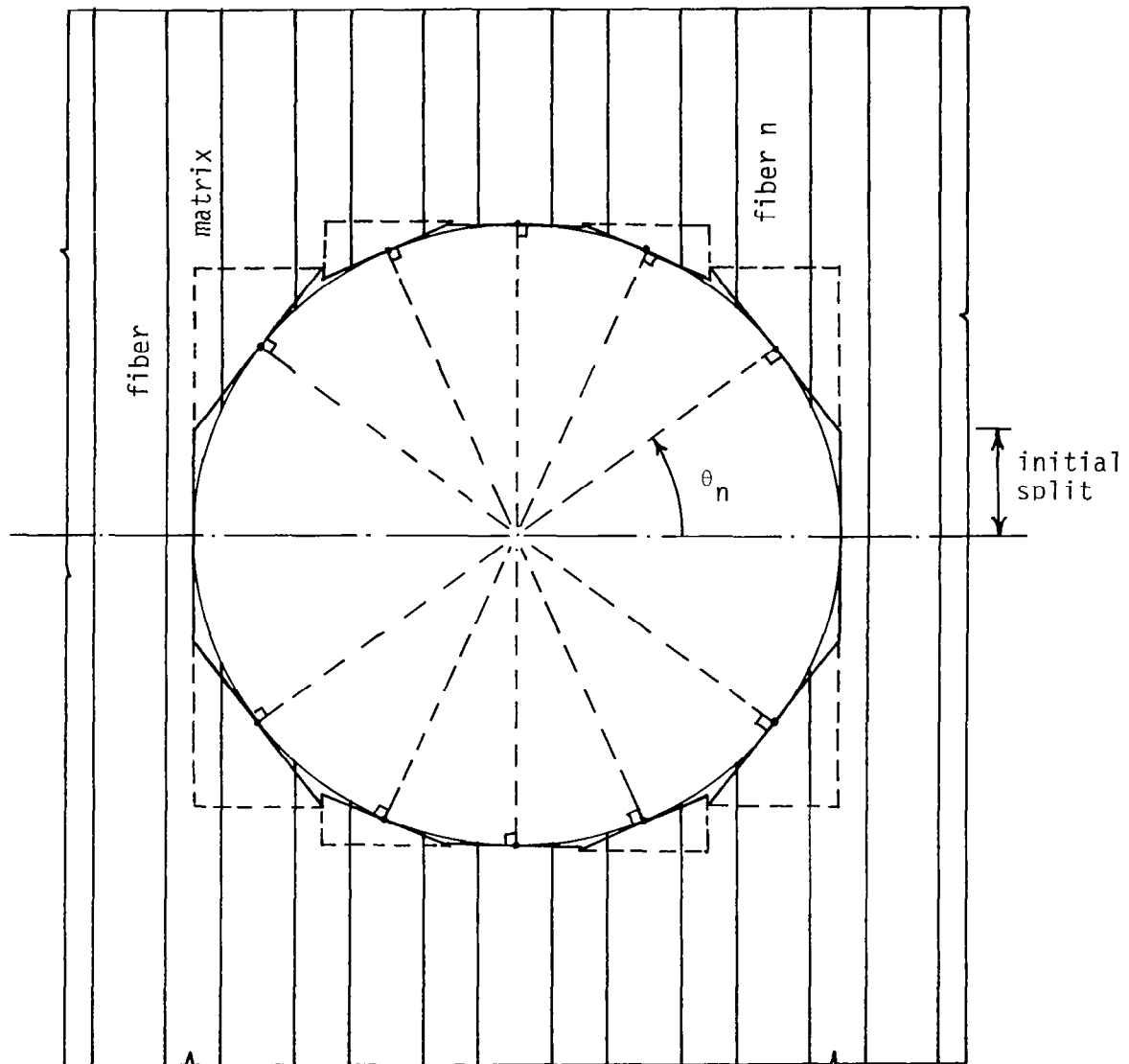


Figure 10. Assembly of boundary elements for the circular cut-out.

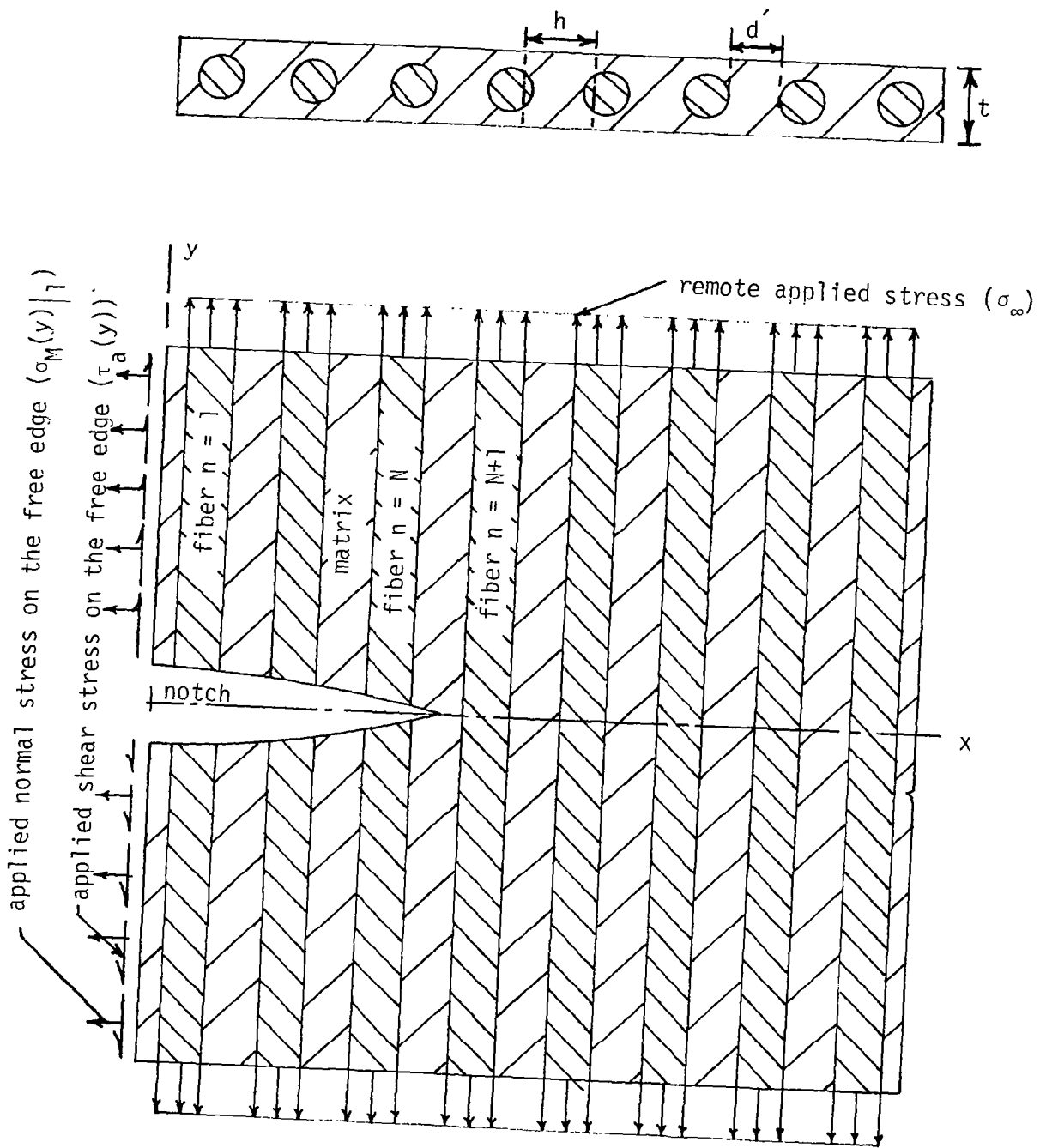


Figure 11. Two-dimensional unidirectional half-plane with broken fibers at the free edge.

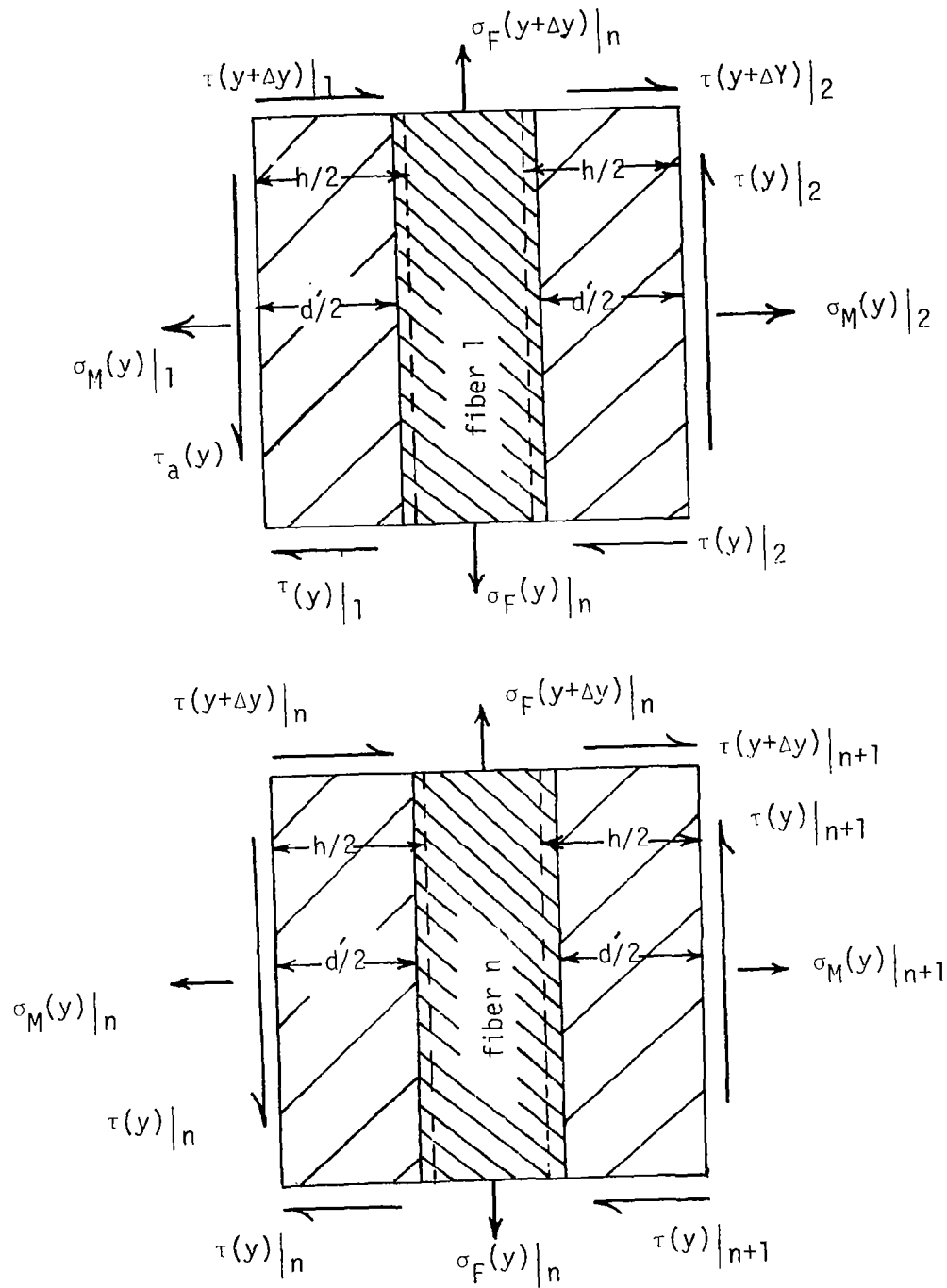


Figure 12. Free-body diagrams of typical elements for the half-plane problem.

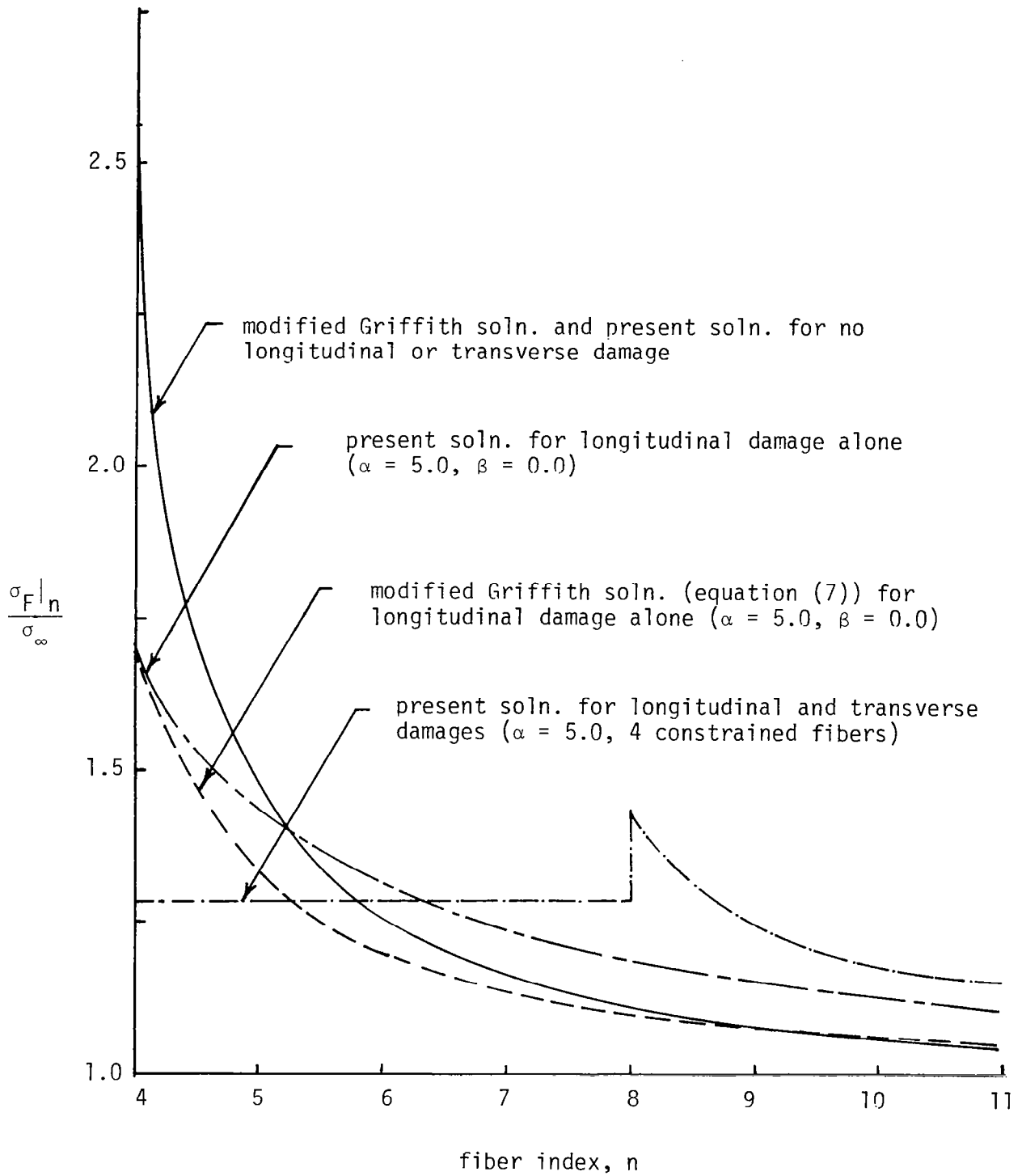


Figure 13. Comparison of notch tip stress distribution for seven broken fibers.

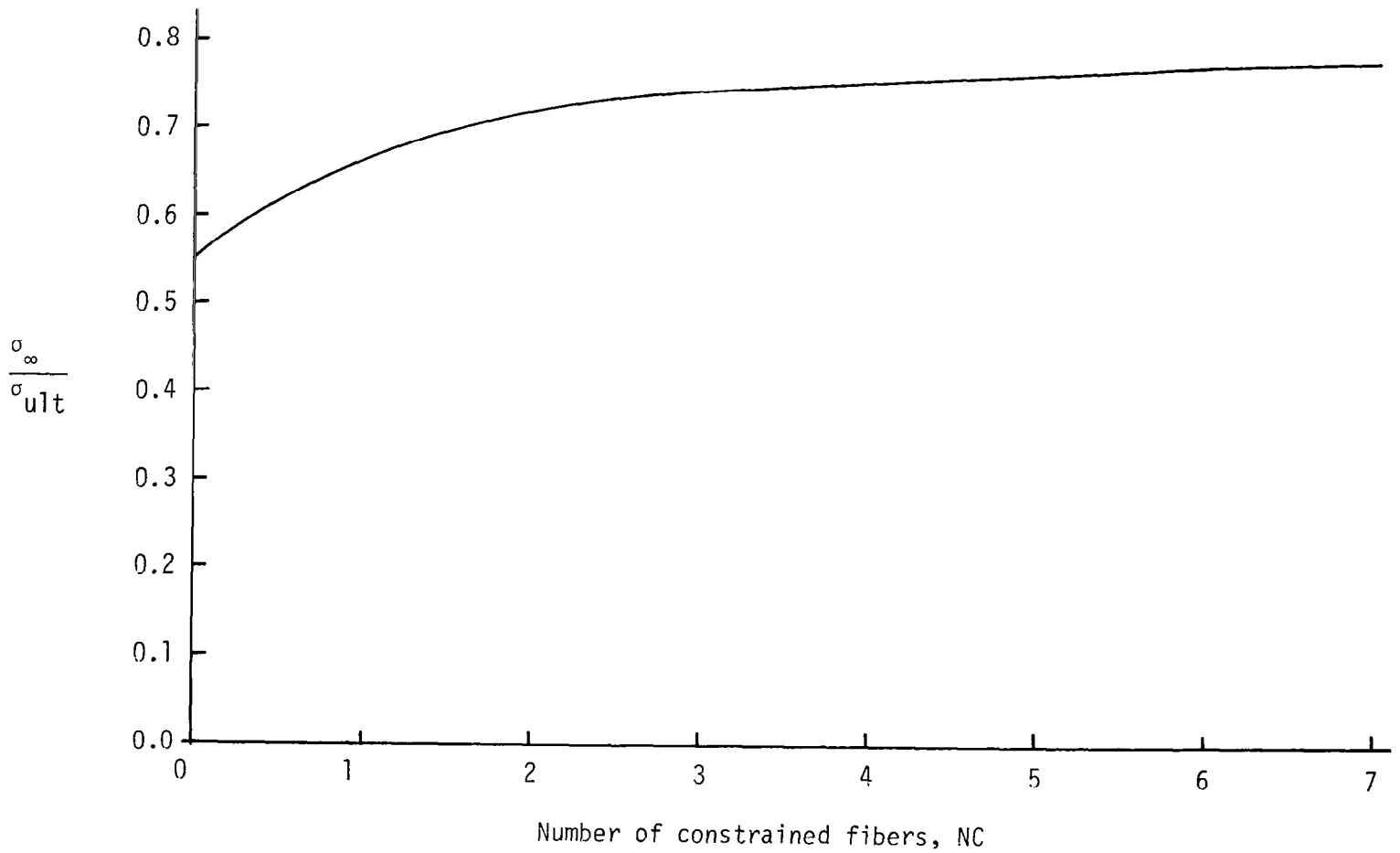


Figure 14. Applied stress as a function of number of constrained fibers in the transverse damage zone for seven broken fibers.

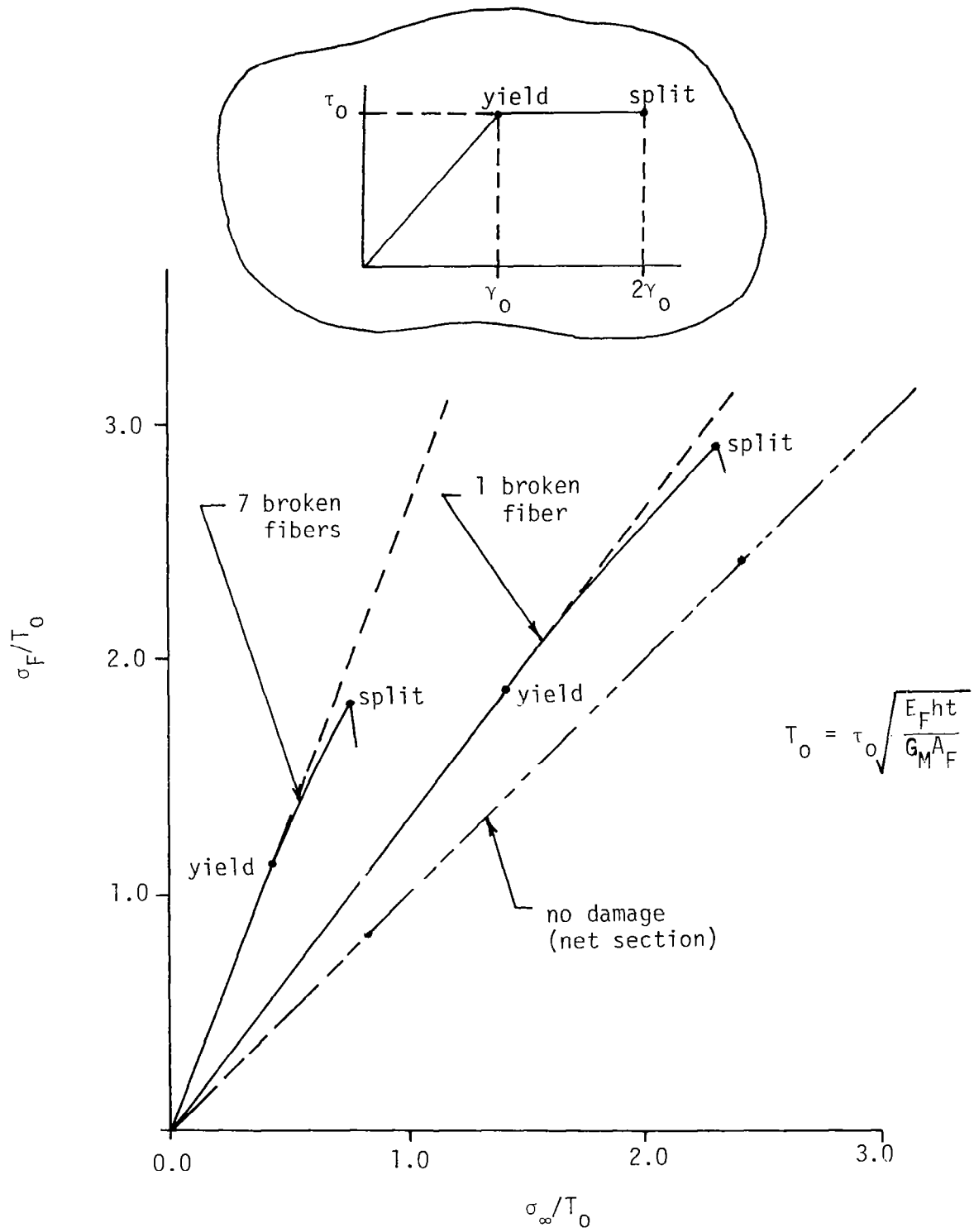


Figure 15. Maximum fiber stress for yielding and splitting.

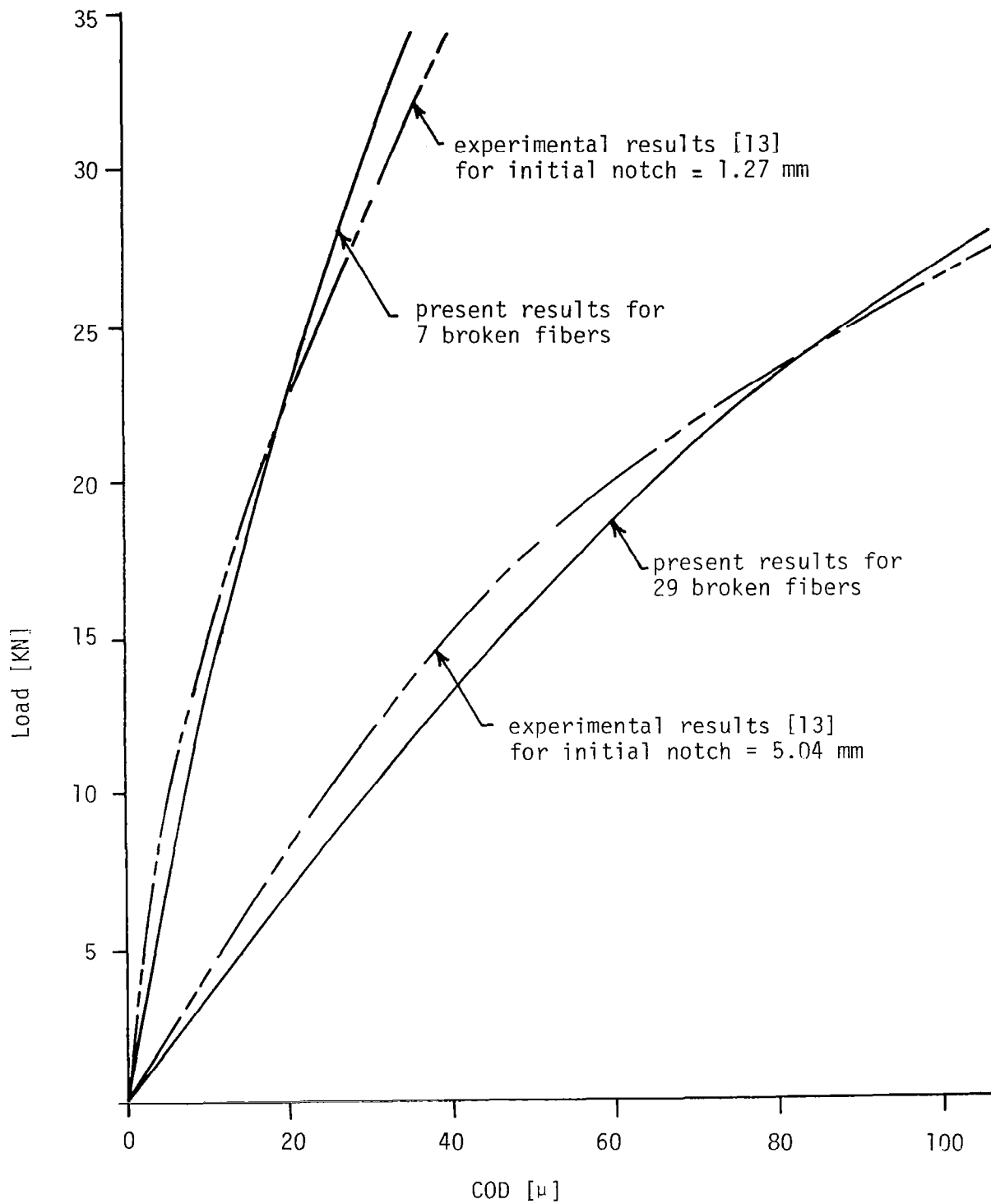


Figure 16. Comparison of present results (longitudinal damage model) with experimental study for a 25.4 mm by 8 ply laminate.

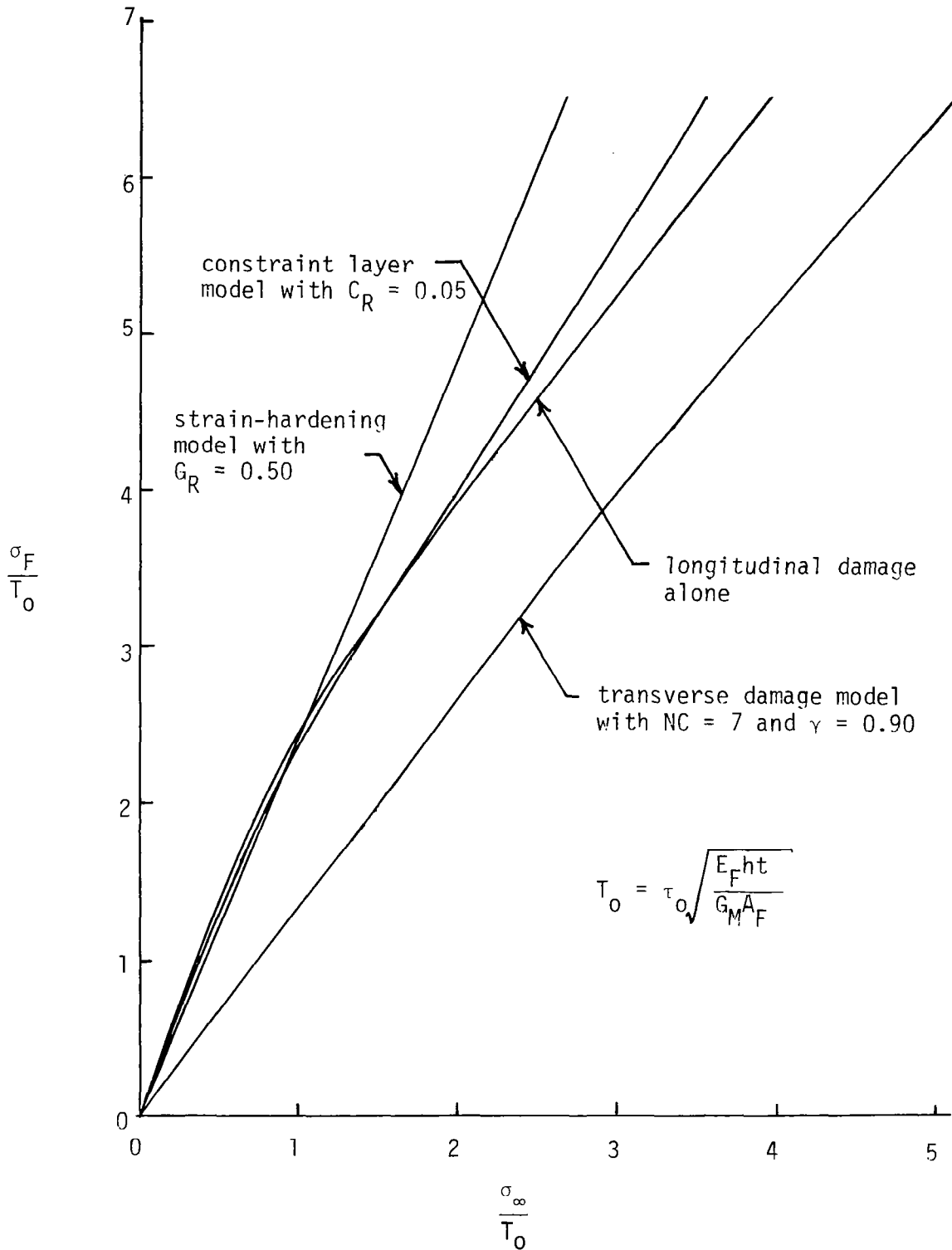


Figure 17. Maximum fiber stress in the first intact fiber at $\eta = 0.0$, as a function of applied stress for the case of no splitting and 7 broken fibers.

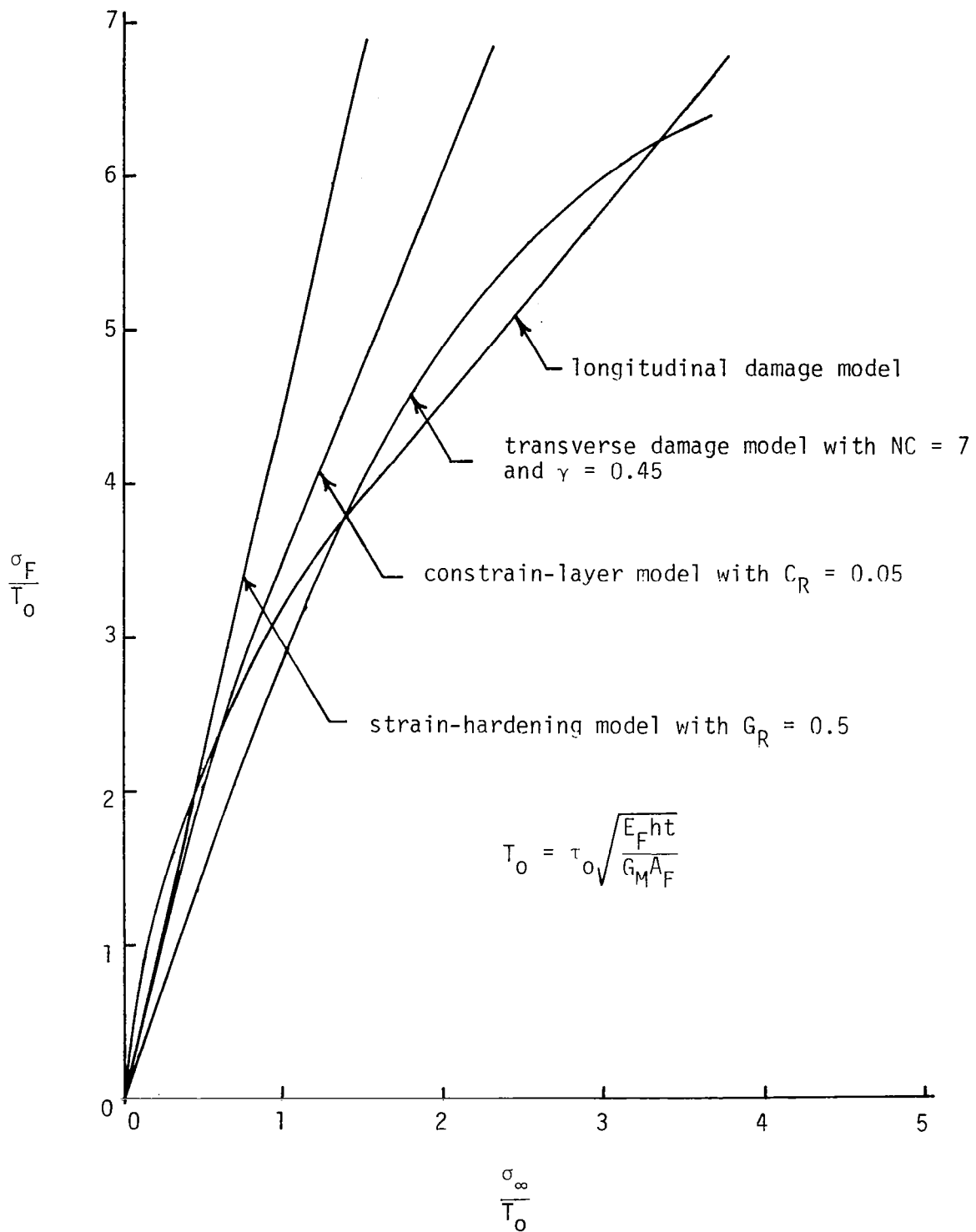


Figure 18. Maximum fiber stress in the first intact fiber at $\eta = 0.0$, as a function of applied stress for the case of no splitting and 29 broken fibers.

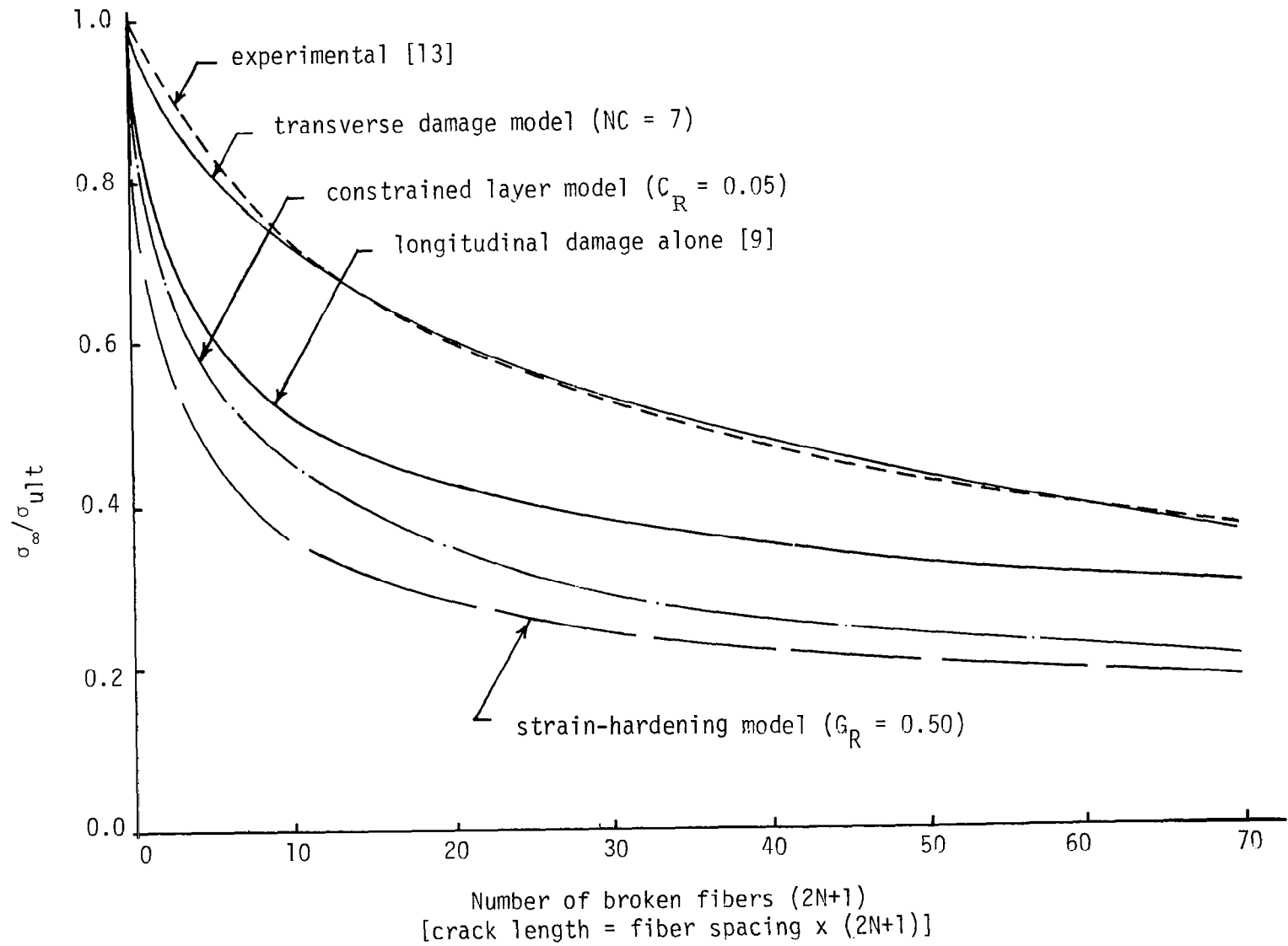


Figure 19. Strength curve: Applied stress as a function of number of broken fibers.

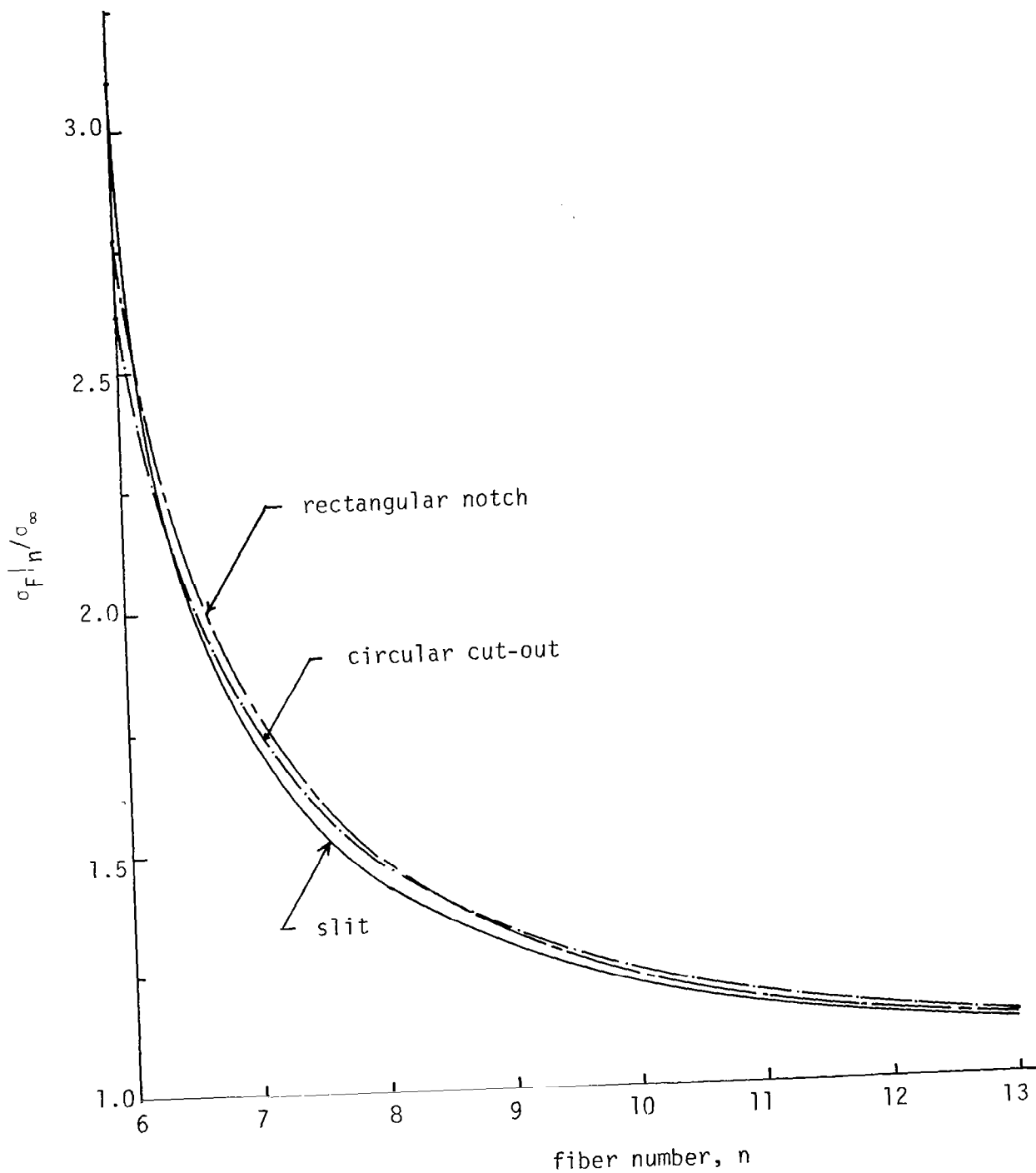


Figure 20. Comparison of notch tip stress distribution for various geometries for eleven broken fibers and no longitudinal and transverse damage.

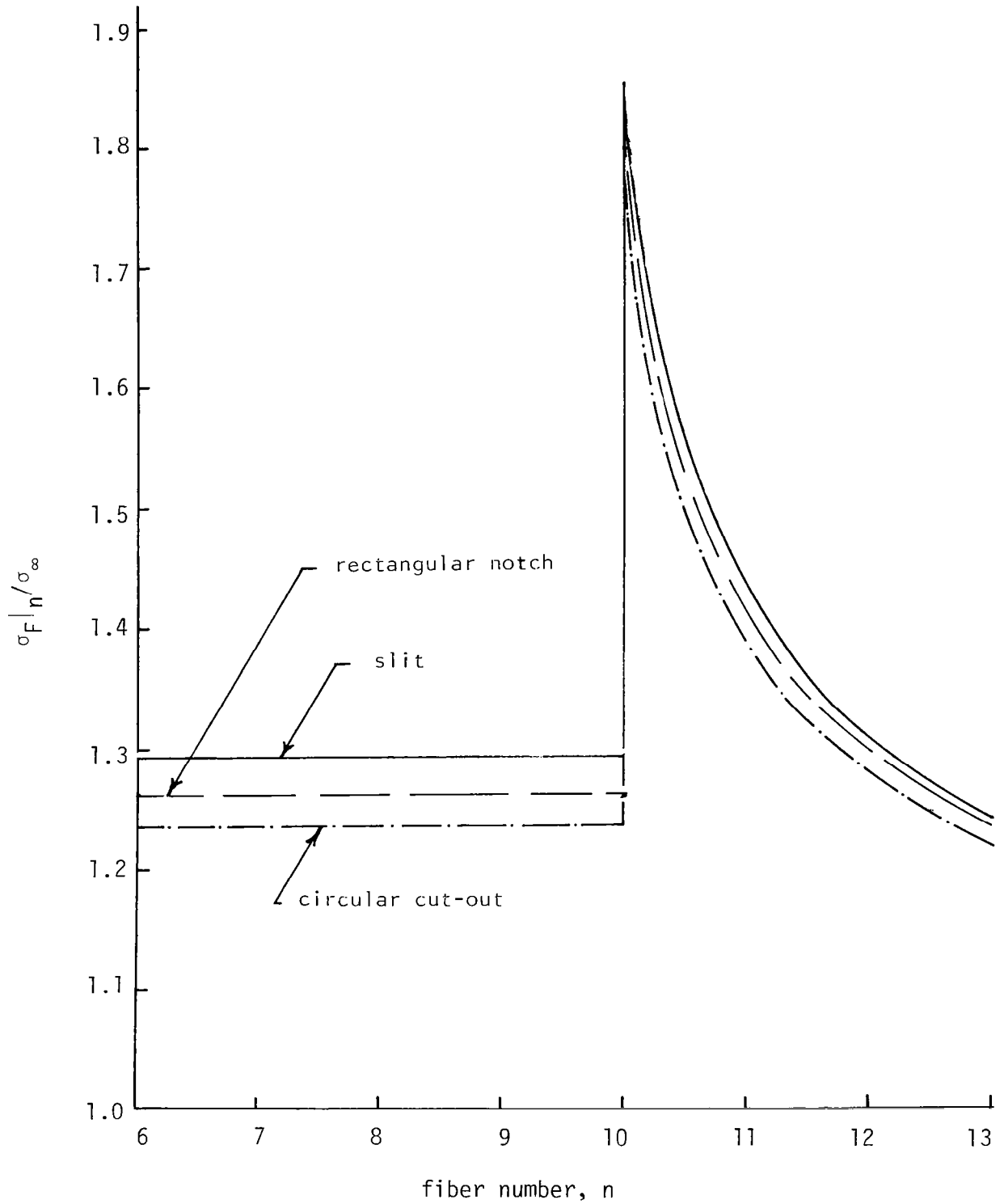


Figure 21. Comparison of notch tip stress distribution for various geometries for eleven broken fibers in the presence of longitudinal and stable transverse damage.

| | | | | | |
|---|--|--|---|--|------------------|
| 1. Report No. NASA CR-3453 | | 2. Government Accession No. | | 3. Recipient's Catalog No. | |
| 4. Title and Subtitle MATHEMATICAL MODELING OF DAMAGE IN UNIDIRECTIONAL COMPOSITES | | | | 5. Report Date August 1981 | |
| | | | | 6. Performing Organization Code | |
| 7. Author(s) James G. Goree, Lokeswarappa R. Dharani, and Walter F. Jones | | | | 8. Performing Organization Report No. | |
| | | | | 10. Work Unit No. | |
| 9. Performing Organization Name and Address Clemson University Department of Mechanical Engineering Clemson, South Carolina 29631 | | | | 11. Contract or Grant No. NSG-1297 | |
| | | | | 13. Type of Report and Period Covered Contractor Report | |
| 12. Sponsoring Agency Name and Address National Aeronautics and Space Administration Washington, DC 20546 | | | | 14. Sponsoring Agency Code 505-33-33-05 | |
| | | | | | |
| 15. Supplementary Notes Langley Technical Monitor: Clarence C. Poe, Jr. Final Report | | | | | |
| 16. Abstract A review of some approximate analytical models for damaged, fiber-reinforced composite materials is presented. Using the classical shear-lag stress-displacement assumption, solutions are presented for a unidirectional laminate containing a notch, a rectangular cut-out, and a circular hole. The models account for longitudinal matrix yielding and splitting as well as transverse matrix yielding and fiber breakage. The constraining influence of a cover sheet on the unidirectional laminate is also modeled. For ductile-matrix composites like boron/aluminum, the model with longitudinal matrix yielding and transverse notch extension agrees best with experimental results. The cover sheet and/or strain-hardening matrix has minor influence. In the case of brittle-matrix composites like graphite/epoxy, longitudinal splitting is the dominant form of damage. Very little difference is found between the results for the notch, rectangular cut-out, and circular hole. In all cases, the presence of longitudinal or transverse damage significantly reduces the stress concentration and gives a much more uniform stress state in the unbroken fibers than a square-root singularity. The formulation of the problem for an edge notch in a unidirectional half-plane with no additional damage is also developed; but, numerical results are not given. This solution forms the basis for the general problem of adjoining half-planes of different fiber-matrix properties. | | | | | |
| 17. Key Words (Suggested by Author(s)) Composite materials Fracture Shear-lag analysis Matrix yielding and splitting Notch strength | | | 18. Distribution Statement Unclassified - Unlimited Subject Category 24 | | |
| 19. Security Classif. (of this report) Unclassified | | 20. Security Classif. (of this page) Unclassified | | 21. No. of Pages 101 | 22. Price A05 |